AN INVESTIGATION OF THE OMEGATRON TYPE MASS SPECTROMETER

Thesis by

Hardy C. Martel

In Partial Fulfillment of the Requirements

For the Degree of

Doctor of Philosophy

California Institute of Technology

Pasadena, California

1956

ACKNOWLEDGEMENT

The author wishes to express his sincere thanks to Professor R. V. Langmuir for his invaluable aid and assistance in carrying out the research reported here. Part of the work reported here was carried out while the author held a Fellowship from the Radio Corporation of America.

In addition, the author wishes to thank his wife for her understanding and consideration both during the research itself and in the preparation of this thesis.

ABSTRACT

An Omegatron type mass spectrometer has been investigated both theoretically and experimentally to determine its detailed operation and limitations. Resolution, peak height, shape and frequency have been calculated theoretically and compared experimentally. A method is given for sketching ion trajectories in the nonlinear case (e.g., with space charge). Using this method, it is shown that a small amount of space charge will seriously hamper the operation of the Omegatron in that it will limit the maximum excursion of a resonant ion and thus limit the possible resolution. It is shown that under normal operating conditions a trapping voltage is necessary to maintain ion collection efficiency, and that this trapping voltage causes a space charge sufficient in size to result in nonlinear ion trajectories and poor operation.

It is concluded that in order to get good operation of the Omegatron some method will have to be found for eliminating the space charge or its effects. Several possibilities for doing this are suggested, the most intriguing one being to use a dipole type of RF electric field rather than a uniform one.

TABLE OF CONTENTS

CHAPTER I

INTRODUCTION

The Omegatron. The Omegatron is an RF type of mass spectrometer which employs the cyclotron resonance phenomena of ions in a magnetic field. In the Omegatron, ions are caused to spiral under the influence of an RF electric field, and those ions that are in resonance with the electric field spiral outward until they strike a collector plate and record their presence as a current. The big advantages of the Omegatron, at least as far as the simple theory is concerned, are:

(a) There are no slits to define a beam and so no critical dimensions.

(b) Mass is measured in terms of frequency and the magnetic field. With O_{16} as a standard, the measurement is strictly frequency, which is generally very easy to measure.

(c) High resolution is obtained by a small RF voltage and only moderate magnetic fields are necessary.

(d) Very high sensitivity is available because practically all the ions produced can be made to go to the collector.

(e) The whole Omegatron is a very simple, compact mechanical structure, being easily contained in a cube of one inch sides.

From the advantages, it appears the Omegatron should be a panacea among spectrometers. It was invented by three men from the National Bureau of Standards, Sommer, Hipple and Thomas (1,2), and used by them

primarily for a high accuracy measurement of the proton magnetic moment. They made no attempt to develop it as a general purpose mass spectrometer or to investigate its limitations, for their work was strictly with masses around hydrogen. Since then, several other people have tried to exploit the Omegatron's advantages. R. L. Bell (3), D. Alpert (4) and A. G. Edwards (5) have all tried to use it as an aid in studying high vacuums with varying degrees of success. The General Electric Company produced a commercial model of the Omegatron and even had it on the market for a few months in early 1955, but it was soon withdrawn for reasons which have never been quite clear. C. E. Berry (30) of the Consolidated Engineering Corporation has published a paper describing the ion trajectories in the Omegatron in detail, but as yet no commercial model of the Omegatron has been produced by this company.

By implication from some of the published work, and by word of mouth from some of the investigators, it appears that the difficulties with the Omegatron are:

(a) While it works fairly well at low masses and under laboratory conditions, it does not behave at all well at the high masses and seems useless above mass 100.

(b) There appears to be considerable anomalous behavior at the low masses and unpredictable DC potentials must be applied to get satisfactory operation. Resonance frequency, size of response, and resolution do not agree with the simple theory.

(c) Only very low electron currents can be used before poor operation occurs.

The purpose of the research reported here is simply to investiggte

in detail from both a theoretical and an experimental point of view the method of operation of the Omegatron. It is hoped that through a better understanding of how the Omegatron operates, a method can be suggested by which its difficulties may be overcome. Two possible reasons that have been suggested for the difficulties with the Omegatron are (a) space charge, and (b) difficulty in controlling ions with very small voltages. These must either be verified or excluded.

History. Mass spectroscopy basically started around 1913 with the work of J. J. Thomson (6) on the deflection of what were then called "positive rays". The rays used by Thomson were the canal rays from a gas discharge tube. A canal ray is a beam of ions of a gas flowing from a hole in the cathode of an ordinary gas discharge tube containing the gas at such a pressure that the Crooke's dark space in front of the cathode is several centimeters long. The ray thus contains ions of the gas with velocities spread over a wide range. Thomson took a canal ray and deflected it with a magnetic and an electric field which were parallel to each other, perpendicular to the ray, and extended over a small region. The deflection was measured at a distance from the fields by letting the ray travel in vacuo to strike a photographic plate mounted perpendicular to their original direction. The deflection parallel to the fields is due to the electric field only and is proportional to qE/mv^2 where q, m and v are the charge, mass and initial velocity of the ion and E is the magnitude of the electric field. The deflection perpendicular to the fields is due to the magnetic field and is proportional to qB/mv where B is the magnetic field strength. For a ray of the same ions with different velocities the deflections thus make a parabolic trace on the photographic plate. For ions of a different mass the trace

is still parabolic but a different parabola. Thomson observed parabolic traces which were reasonably sharp and thus concluded that atoms of a given kind all have the same mass and furthermore that the masses come essentially in integral values only.

This general method of analysing the rays was rendered more precise by Aston (7) some six years later who devised a way of getting longer deflections while at the same time bringing all ions with a given q/m ratio to a focus (rather than having them spread out in a parabola).

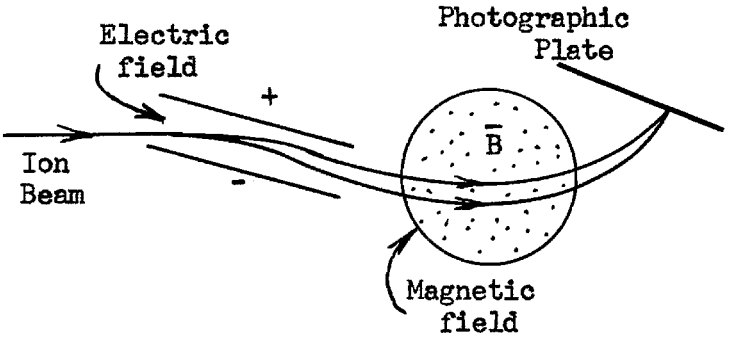

Fig. 1. Aston's Spectrograph.

Aston's mass spectrograph consisted of first deflecting the ions in an electric field and then subsequently reversing the deflection with a magnetic field. Ions of different velocities spread out under the influence of the electric field but are focused by the magnetic field to converge at the photographic plate (see Fig. 1). Ions of different mass are focused at a different place on the plate, and fortunately, by proper design, the locus of focal points for different masses can be made to fall approximately on a straight line so the photographic plate can be flat. From the known dimensions of the apparatus and the electric and magnetic fields the mass of the ions can be calculated. By refining his equipment, Aston was able to show that the masses of atoms were almost, but not quite, integers, and this stirred great interest in more precise types of spectrometers.

Dempster invented the first of the now common 180° mass spectrometers.

His apparatus (8) consisted of an ion source and an accelerating electric field producing a high velocity, essentially mono-energetic ion beam, the beam being formed by a slit in the accelerating electrode. The ion source itself was actually a heated salt of the element under consideration which released ions of fairly small initial velocity which were then accelerated. After acceleration, the ions were deflected by a uniform magnetic field as in Fig. 2. In the magnetic field an ion travels a circle of radius $r = mv/qB = \sqrt{2mV/qB^2}$; thus the radius varies in proportion to the square root of the mass. Dempster used slits to define a path of specified radius and thus allow only ions of a specified mass through. After an ion had traveled a half circle, it was collected on a plate and the current registered on an electrometer. To first order, ions entering the magnetic field with velocities in different directions are focused at the exit slit, a desirable condition to keep resolution and sensitivity high. By varying the accelerating potential V , the ion velocity could be varied and thus ions of different mass would travel the semi-circular path. Plotting the collected ion current as a function of accelerating potential showed a series of sharp maxima, each corresponding to a particular value of q/m.

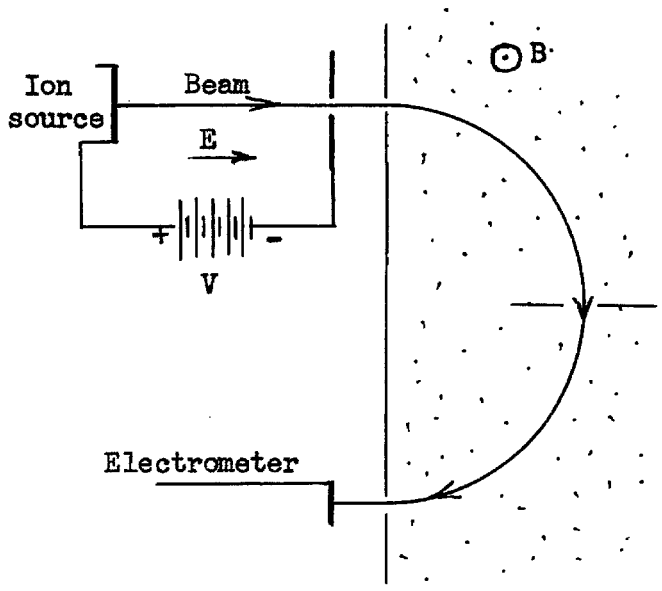

Fig. 2. Dempster's Spectrometer

More recently, Bainbridge (9) has devised a spectrometer of high

resolution and precision which has the big advantage of a linear mass scale. In his equipment positive ions are injected with a range of velocities into a region of crossed electric and magnetic fields. Thus ions with a velocity $v = E/B$ travel through this region under no forces (thus a straight line) while ions with other velocities are deflected and removed from the beam. The region of crossed fields thus serves as a velocity selector, passing only ions with a predetermined velocity. After the velocity selector, the ions then travel in a circular path of radius proportional to their mass under the influence of only the magnetic field. After a half circle, they strike a photographic plate where they leave an image. The images on the plate from various mass ions (assuming the same charge) are spaced linearly along the plate in proportion to their mass.

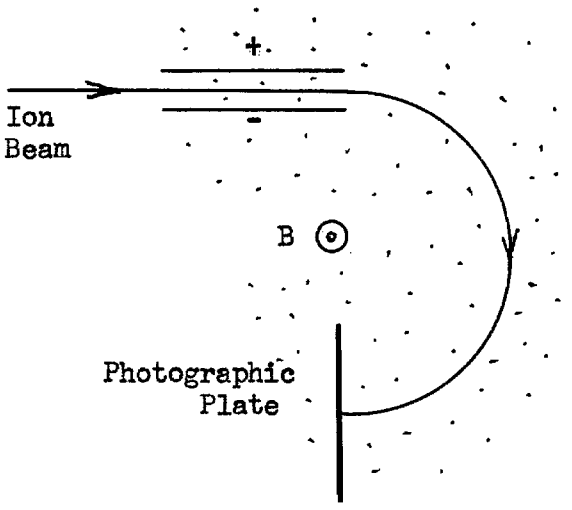

Fig. 3. Bainbridge's Spectrograph.

A form of spectrometer of considerable interest is the crossed field type first introduced by Bleakney and Hipple (10) around 1938. For this spectrometer ions travel a trochoidal path in mutually perpendicular uniform magnetic and electric fields.

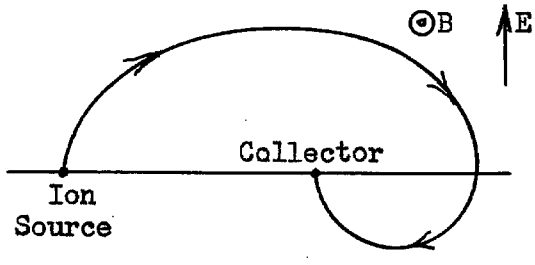

Fig. 4. Ion path.

The interesting point here is that no matter what their initial velocity is (either in magnitude or in direction), all ions from the source are focused to a point (actually an image of the source defining slit); thus ion collection efficiency and resolution can be very high. The distance between the ion source and the first focal point is a function of the mass of the ion, thus effecting spatial mass separation. This idea of course could be extended to multiple loop trochoidal paths with the possibility of getting still higher resolution.

In recent years there has been a great deal of work on mass spectrometers in several directions. For laboratory research tools effort has been toward making them have greater resolution and precision. For general analytical work in the field they should be simple, reliable, easy to operate and still have fairly high sensitivity and resolution. For leak detection applications sensitivity is most important while only moderate resolution and precision are needed. A great many different ways have been found for arranging electric and magnetic fields so that a separation of ions of different q/m results. Far too many ways are known to catalogue them here in any detail; however, the general methods that are employed can be outlined briefly.

Essentially there are three quantities - velocity, momentum and energy - which can be measured for an ion. Only two of these three are needed to determine the mass, and spectrometers can be listed according to which two they use. It should be pointed out here that spectrometers can also be classified according to the type of focusing they use. There are three basic types of focusing: (1) <u>direction focusing</u>, i.e., focusing of ions homogeneous as to mass and velocity but of different initial direction; (2) <u>velocity focusing</u>, i.e., focusing of ions homogeneous as

to mass and direction but of different initial velocity; and (3) double focusing, i.e., focusing of ions homogeneous in mass but of varying velocities and directions. It is customary in mass spectroscopy to use focusing systems equivalent to cylindrical lenses, though a few systems achieve focusing analagous to spherical lenses, i.e., point to point focusing. Focusing can be perfect, meaning it is exact for all ranges of the variable velocity of direction, or it can be first or higher order focusing, meaning it is only approximate to first or higher order in the variable. Because the type of focusing strongly determines the possible resolution, focusing is a very reasonable way to classify spectrometers. But when so classified the list becomes rather extensive and since it can be found in the literature (11) it will not be given here. More complete descriptions of the history and recent developments in mass spectroscopy can be found in several texts (12,13). Classification according to the two quantities measured leads to the following:

(1) Momentum-energy selection. This class is typified by the spectrometers of Thomson, Aston and Dempster in which energy is measured by an electric field and momentum by a magnetic field. The most common types of spectrometers, the 60°, 90° and 180° types, fall into this class (14-20), and in these a mono-energetic ion beam is produced by an accelerating electric field and then momentum is measured by the radius of the beam while deflecting through the specified angle in a magnetic field. Focusing in these types is first order in direction only, and always the ion beam is defined mechanically, i.e., by slits.

(2) Energy-velocity selection. This class generally uses a mono-energetic beam and a method of velocity selection. The latter may be by crossed electric and magnetic fields (21,22), RF fields (23,24,25)

or by a pulsed beam technique (26,27). The RF field and pulsed beam techniques lead to spectrometers which are usually called "time of flight" types.

(3) Momentum-velocity selection. There are three quite different types of spectrometers which fall in this class. The first is typified by Bainbridge's setup in which velocity was selected by a Wien filter (crossed electric and magnetic fields) and momentum was measured by radial magnetic deflection. The second and third both fall into the time of flight class. In one (28,29) a pulsed beam of ions is sent into an homogeneous magnetic field, the radial magnetic deflection giving momentum and the time for n revolutions giving velocity. In the other, momentum and velocity are almost simultaneously obtained by measuring the cyclotron resonance frequency of an ion in a homogeneous magnetic field. This latter one has been given the name Omegatron by its inventors, Thomas, Hipple and Sommer of the National Bureau of Standards, and it is the subject of this dissertation.

The experimental Omegatron. In its embodiment used for the experimental work to be reported here, the Omegatron is shown in Fig. 5. It consists of a one inch cube of 0.020 inch stainless steel plates in a uniform magnetic field. The top and bottom plates are called the RF plates and serve to produce a vertical electric field which varies sinusoidally in time. They are driven by an RF signal generator of variable frequency. In addition, DC potentials can be applied to these plates to produce a vertical DC electric field for the purpose of "walking" the ions either towards or away from the collector. The two plates called Z plates are supplied with DC potentials whose prime purpose is to provide an inward directed electric field to keep the ions from

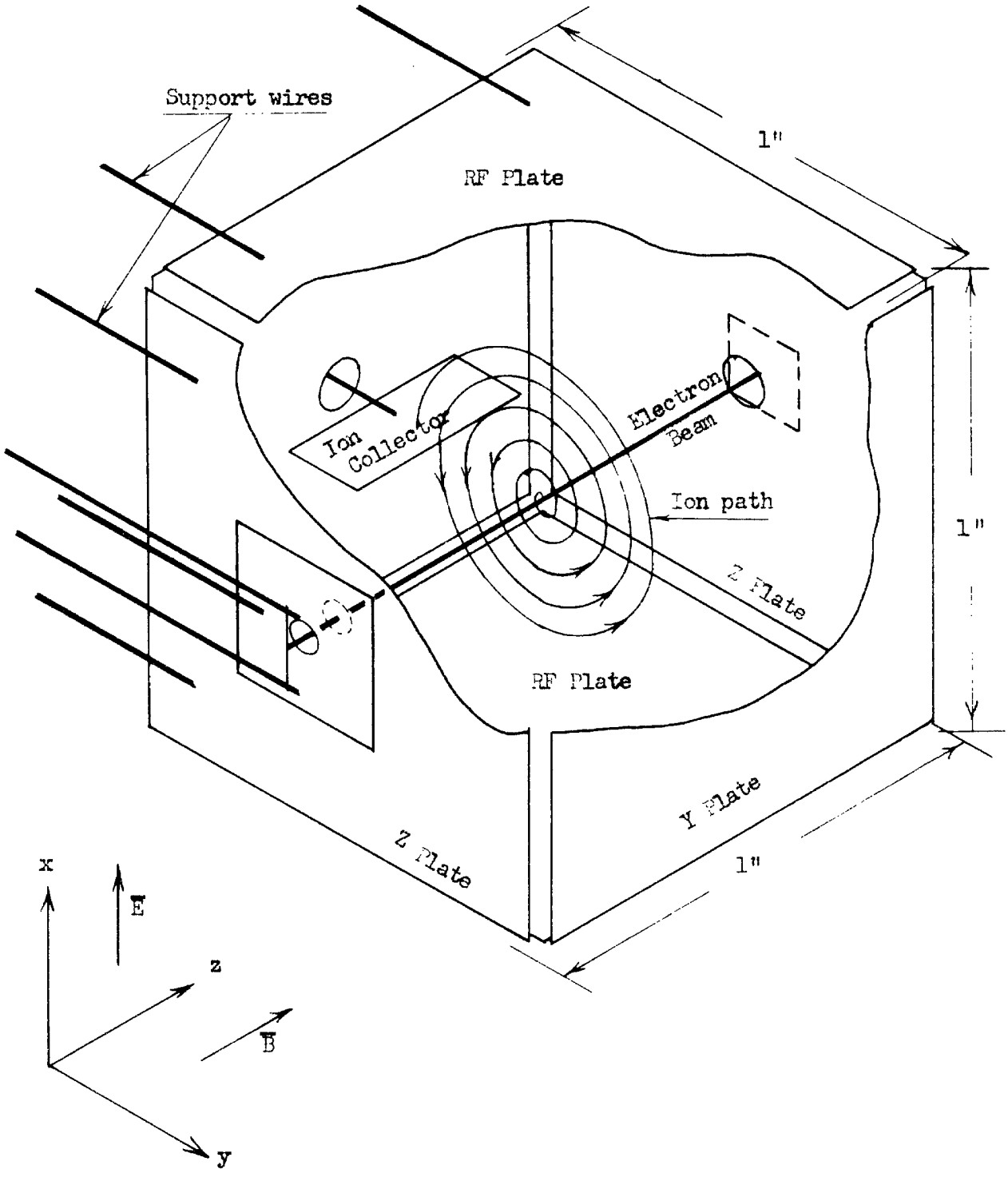

Fig. 5. Omegatron

drifting out of the useful region. This field is usually called a "trapping field" and the associated voltage a "trapping voltage". The two Y plates serve primarily as shielding for the interior of the cube and so are normally grounded but can also have potentials applied if needed. At the left is a 0.003 inch tungsten filament which is heated to provide a supply of electrons. Next is an electron accelerating plate which has a 1/16 inch diameter hole to form the electron beam. This plate is normally run at 67 volts plus with respect to the filament. The electron beam travels through the cube and in the process some of the electrons collide with gas molecules and ionize them. The majority of the electrons travel without collisions and pass through a hole in the far Z plate and are collected on an electron collector plate which is run a few volts positive (to suppress secondary emission). The ions that are formed by the electron beam start essentially at rest (actually have thermal velocities) along the beam and are accelerated by the electric field to travel spiral paths (see later analysis). Those ions in resonance spiral out far enough (electron beam to collector spacing 3/8 inch) to hit the ion collector, where they represent a current flow which is measured by a sensitive electrometer.

A block diagram of the electronics associated with the Omegatron is shown in Fig. 6. For convenience in operation, the frequency of the RF is continuously swept over a small range. The electrometer output is applied to the vertical deflection system of an oscilloscope while the spot is deflected horizontally in synchronism with the sweep oscillator. The scope then displays collected ion current versus frequency and so a resonant ion produces a peak in the trace. The upper trace in Fig. 7 shows (reading from left to right) mass 16, 17, 18 and

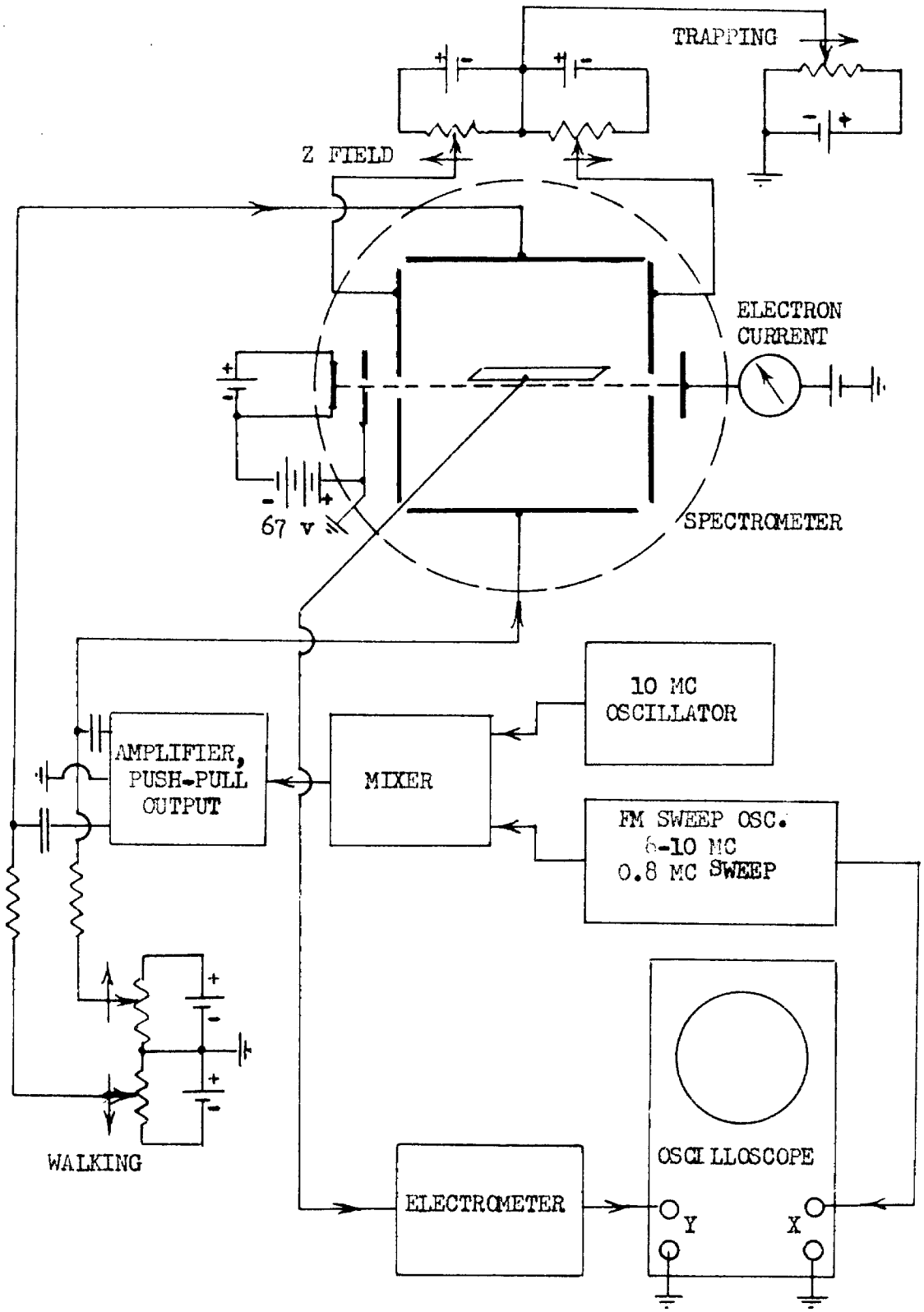

Fig. 6. Block diagram.

19 peaks while the lower trace has a highly compressed frequency scale to show masses 16, 17, 18, 19, 28, 32, 44, 50 and some higher mass peaks that are not separated.

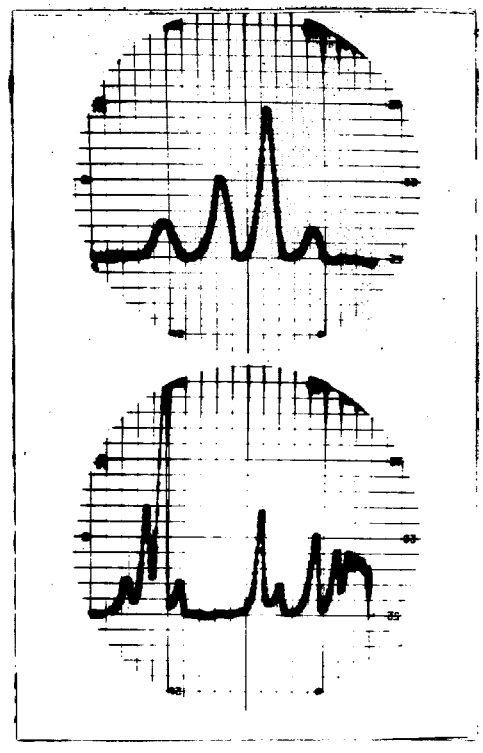

Fig. 7. Omegatron peaks.

Typical operating conditions. To get order of magnitude data for some of the theoretical results that follow, it will be convenient to have a set of typical operating conditions. These conditions were found experimentally to produce a useful peak size in actual operation around mass 18:

B = 3500 gauss	RF = 1.8 volts RMS
Electron current = 0.05 μ amps	Walking = 0 volts
Trapping = 0.25 volts	Z field = 0 volts

Electron accelerating voltage = 67 volts

Electron collector voltage = 6 volts

Peak ion current = 10^{-12} amps

Background pressure = 2×10^{-6} mm of Hg.

The RF voltage quoted above corresponds to a peak electric field strength of 100 volts/m if one neglects any fringing of the electric field.

CHAPTER II

THEORETICAL RESULTS

Problem. In its most simplified form, the essence of the Omegatron is indicated in Figure 8. A point mass-charge particle starts from rest at the origin and moves in a time-invariant uniform magnetic field perpendicular to the paper and a sinusoidally time-varying uniform electric field along the x axis. The problem is, what is its trajectory? This problem is a two dimensional one - everything is taken uniform in the z direction (perpendicular to the paper).

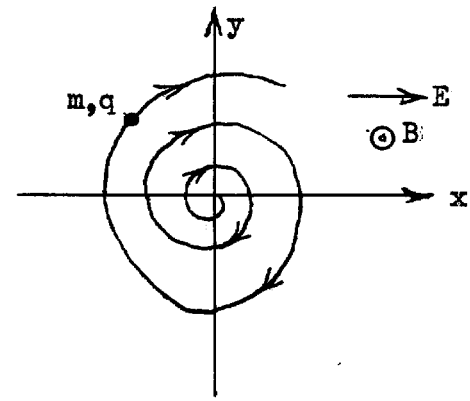

Fig. 8. Simplified problem.

Of the various methods of solution available for this problem, there are two general approaches of interest. The first approach is a straightforward solution in fixed cartesian coordinates, while the second involves transforming to a rotating coordinate system before solving the equations of motion. The latter approach provides several types of solutions through different velocities for the rotating system.

Cartesian coordinates. In cartesian coordinates, the equations of motion of a point mass-charge particle, mass m and charge q, are

$$F_x = m\ddot{x} = q\left[E_m \sin(\omega t + \phi) + B\dot{y}\right], \qquad \text{II-1}$$

$$F_y = m\ddot{y} = -q\,B\,\dot{x} \quad , \qquad \text{II-2}$$

where the electric field is $\bar{E} = E_x = E_m \sin(\omega t + \phi)$ and B is the magnetic field. The solution to this problem is straightforward Assuming the particle starts at the origin at $t = 0$ with zero velocity,

$$y = \frac{E_m}{B(\omega^2 - \omega_c^2)}\left[+\sqrt{\omega_c^2 + (\omega^2 - \omega_c^2)\cos^2\phi}\ \cos\ (\omega_c t + \gamma) \right.$$

$$\left. - \frac{\omega_c^2}{\omega} \cos(\omega t + \phi) \right] - \frac{E_m}{B\omega} \cos\phi \quad , \qquad \text{II-3}$$

$$x = \frac{E_m}{B(\omega^2 - \omega_c^2)}\left[-\sqrt{\omega_c^2 + (\omega^2 - \omega_c^2)\cos^2\phi}\ \sin(\omega_c t + \gamma) \right.$$

$$\left. - \omega_c \sin(\omega t + \phi) \right] , \qquad \text{II-4}$$

where $\omega_c = qB/m$ and $\gamma = -\tan^{-1}\left(\frac{\omega_c}{\omega} \tan\phi \right)$. It is clear from these results that for an electric field frequency ω near the cyclotron resonance frequency ω_c the maximum excursion of an ion becomes very large. At resonance the ions spiral outward indefinitely. A rather complete discussion of these results has been given by C. E. Berry (30), where they are interpreted in terms of a coordinate system rotating at the electric field frequency. The results are the same as those obtained by solving the problem completely in the rotating coordinate system as will be done later and so will not be given here.

By writing the equations of motion II-1 and II-2 with the driving force on the right hand side it is clear that linear superposition of different driving fields is allowed and also that the complete solution to the problem with initial conditions can be obtained by adding the

solution of the same problem with zero initial conditions to the solution of the problem without any driving force but with the actual initial conditions, a procedure very similar to finding the complementary function and the particular integral. In particular, the results II-3 and II-4 can be obtained by superimposing two rotating electric fields with opposite but equal angular velocities ω. Furthermore, for frequencies near resonance the effect of the backwards rotating electric field will be only to add a small perturbation - a jiggle motion - to the paths. Since we are interested only in the average motion of an ion, these jiggles can be neglected and an approximate solution obtained by considering only one of the two component rotating electric fields. Under this condition it is reasonable to consider motion in a rotating coordinate system.

Rotating coordinate system. The vectorial equation of motion for an ion in general is

$$\bar{F} = m\bar{a} = q(\bar{v}x\bar{B} + \bar{E}). \qquad \text{II-5}$$

Relative to a coordinate system with the same origin and rotating with an angular velocity $\bar{\omega}_s$, equation II-5 becomes

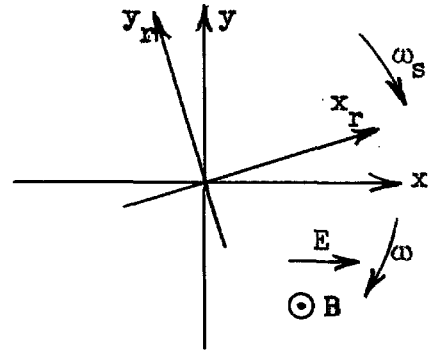

Fig. 9.

$$m(\bar{a}_r + 2\,\bar{\omega}_s x \bar{v}_r + \bar{\omega}_s x(\bar{\omega}_s x \bar{r})) = q(\bar{v}_r x \bar{B} + (\bar{\omega}_s x \bar{r}) x \bar{B} + \bar{E}), \qquad \text{II-6}$$

where the subscript r refers to motion relative to the rotating coordinate system. A more complete derivation of II-6 and the other results in this section may be found in Appendix I. It might be noted that the general method used here is very similar to that involved in Larmor's

Theorem.

The particular problem under consideration is the motion of an ion in an electric field of constant magnitude but rotating in direction in the x-y plane and a uniform magnetic field perpendicular to the x-y plane. In order to write the results in terms of scalar quantities which under normal conditions are positive, the positive directions for the various quantities are assigned as in Fig. 9; thus clockwise angular frequencies for ω and ω_s are positive and B is out of the paper. The cyclotron resonance frequency ω_c as a vector is $\bar{\omega}_c = -q\bar{B}/m$, but here it is treated simply as a scalar number, $\omega_c = qB/m$, which for the +B direction as assigned would also be clockwise if ω_c is positive. There are three cases of interest to consider now and these are when the angular velocity of the rotating coordinate system has a value equal to (a) half the cyclotron resonance frequency ω_c, (b) the electric field frequency ω, and (c) the cyclotron resonance frequency.

(a) $\omega_s = \omega_c/2$. In this case, II-6 becomes much simpler, being

$$m\bar{a}_r = -m\,\omega_c^2\,\bar{r}/4 + q\bar{E}\,. \qquad \text{II-7}$$

This equation describes the motion of an ion under the action of a radial spring from the origin and the original electric field. While the equation itself is now particularly simple because the magnetic field cancelled out, general solutions to this equation are not especially simple, particularly for the case of nonlinear magnetic field variations. Resolving the rotating electric field into components along the relative coordinate axes allows II-7 to be separated into two equations, one involving x_r and one y_r, which places strongly in evidence the resonance character of the solutions.

(b) $\omega_s = \omega$. In this case the coordinate system rotates at a frequency equal to the electric field frequency. In the rotating coordinate system the electric field is stationary and the equation of motion II-6 becomes

$$m\bar{a}_r = q(\bar{v}_r x \bar{B}_1 + \bar{E}) - K\,\bar{r} \qquad \text{II-8}$$

where $\bar{B}_1 = \bar{B}(1 - 2\omega/\omega_c)$ and $K = m\omega(\omega_c - \omega)$. Thus the particle appears to move in a modified magnetic field and under the action of a radial spring from the origin and the now fixed electric field. Though this equation appears more complicated than II-7, it has a fairly simple interpretation. At resonance, $\omega = \omega_c$, the radial spring disappears, $\bar{B}_1 = -\bar{B}$ and the particle travels a cycloidal path with an average motion perpendicular to the electric field. The average motion has a velocity $v = E/B$ while the superimposed circular motion is at frequency ω_c and of radius $r = v/\omega_c$ as in Fig. 10. It will become apparent later that for normal operation with fairly high resolution, the circular motion can be neglected and only the average drift motion is significant.

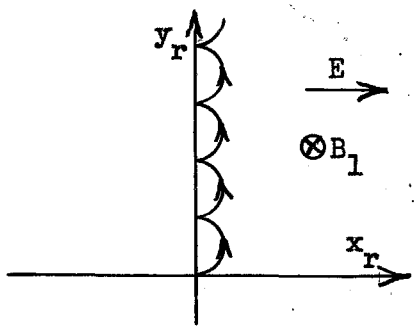

Fig. 10. Resonant ion trajectory.

Off resonance the radial spring must be included, but the problem can be simplified by two more transformations. The first comes about by recognizing that the effect of the radial spring plus the electric field (which is now just a fixed force in the x_r direction) is the same as a radial spring connected not to the origin but to a point on the x_r axis at

$$x_r = x_1 = qE/K \,. \qquad \text{II-9}$$

We can now refer the motion to a new set of coordinates, x_r' and y_r', parallel to x_r and y_r but displaced so their origin is at $x_r = x_1$. The particle now appears to move in a magnetic field B_1 and under the action of a radial spring from the origin of constant K, but the initial conditions now are that it starts with zero velocity at $x_r' = -x_1$, $y_r' = 0$. This new problem can be solved by one further transformation,

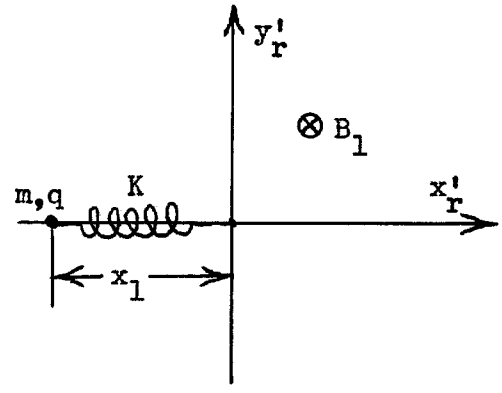

Fig. 11.

and that is to a new coordinate system that gets rid of the radial spring. The new coordinate system, x_r'' and y_r'', is one that rotates clockwise with respect to the primed system at a rate $(\omega_c - \omega)$. In the new coordinate system, the spring disappears (by virtue of the $-\omega$ part of the transformation), what was B_1 becomes the original B in magnitude but reversed in direction (from the combined effect of first a $-\omega$ and then an ω_c transformation), and the particle initial conditions are now $x_r'' = -x_1$, $y_r'' = 0$ and $\dot{x}_r'' = 0$, $\dot{y}_r'' = -(\omega_c - \omega) = -(E/B)(\omega_c/\omega)$. The motion in the double primed system is clearly a circle of radius $r'' = E/B\omega$ (see Fig. 12). In the primed system this becomes an hypocycloid (epicycloid for $\omega > \omega_c$) as shown

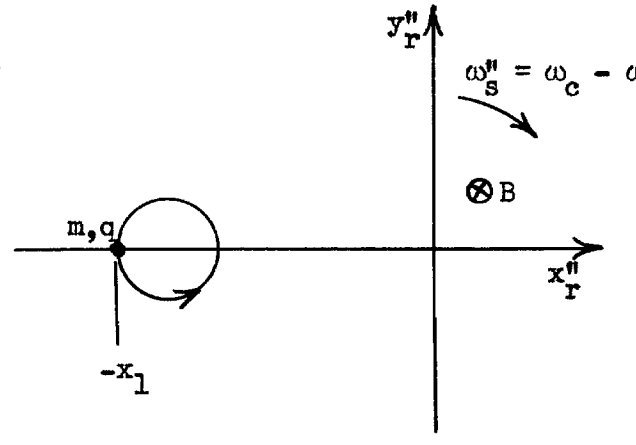

Fig. 12.

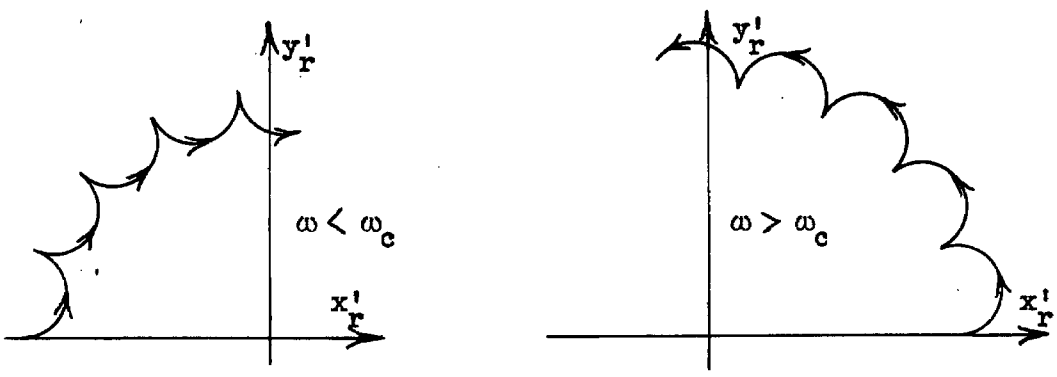

Fig. 13. Trajectories in primed coordinate system.

in Fig. 13, and in the unprimed system (the original rotating coordinate system at the electric field frequency) these cycloids are just displaced as in Fig. 14. Along their path, ions travel with an average velocity $(E/B)(\omega_c/\omega)$ and thus near resonance all ions have an average velocity of about E/B.

Figure 14 shows that for a given electric field frequency, particles of different masses would travel different paths. Those in resonance would travel out the y_r axis with cycloidal motion; those out of resonance would travel circles with a superimposed jiggle motion (actually epi- or hypocycloids), the radius of the circle being smaller the further off resonance. More detailed conclusions from these paths will be drawn later.

(c) $\omega_s = \omega_c$. When the relative coordinate system rotates at a frequency equal to the cyclotron frequency, II-6 becomes

$$m\bar{a}_r = q(-\bar{v}_r x \bar{B} + \bar{E}) \quad . \qquad \text{II-10}$$

Thus the motion is apparently that of a particle in a magnetic field of the same magnitude but reversed direction along with the original electric field. This approach has some advantages for interpreting the

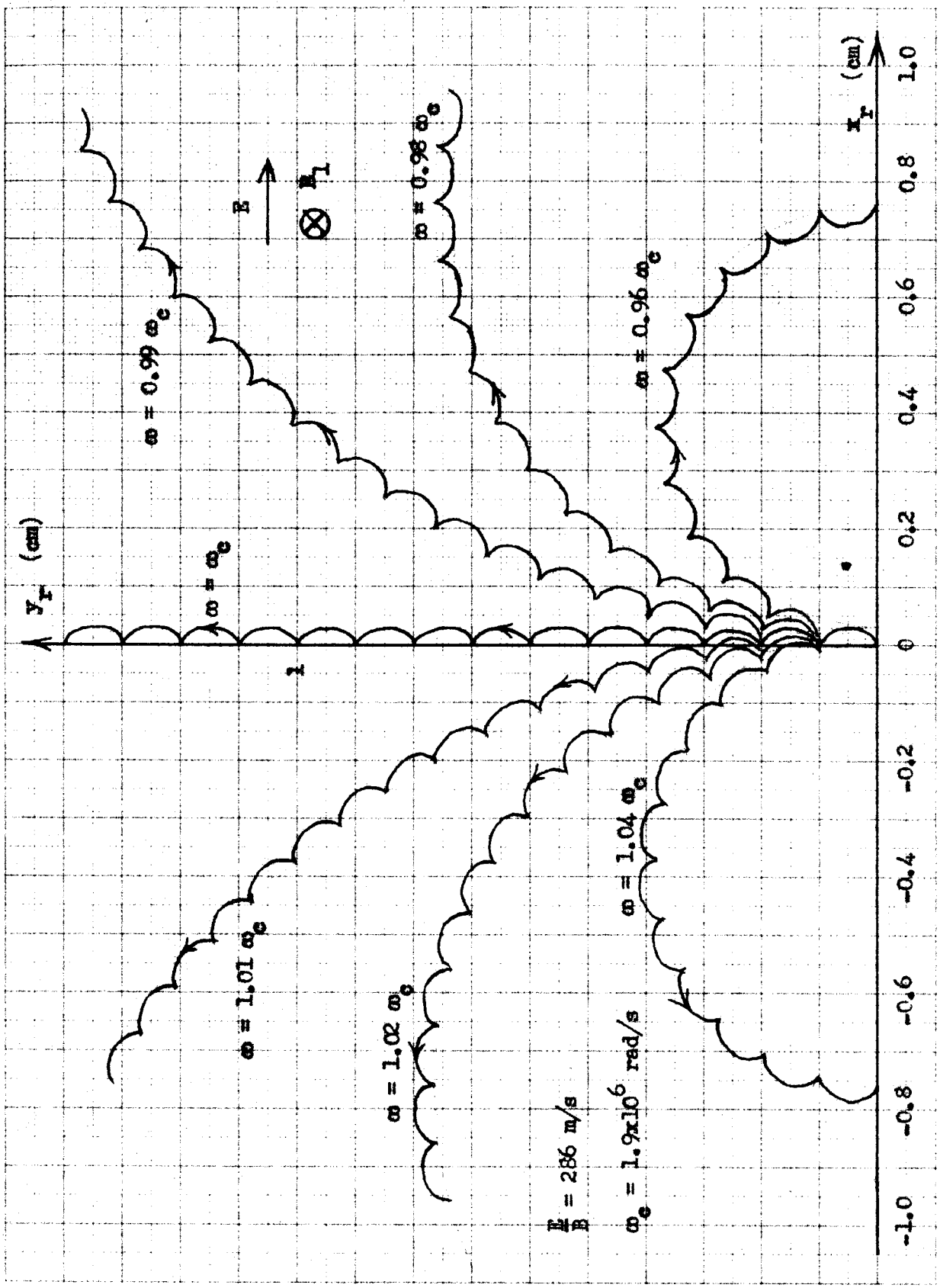

Fig. 14. Ion trajectories in rotating coordinate system.

results near resonance. In the latter case, the electric field is rotating very slowly with respect to the relative coordinate system. The motion of a charged particle in a fixed electric field is cycloidal with average drift perpendicular to the electric field and thus in a slowly rotating electric field the particle traces out a circle for its average path. This then gives the same results as depicted in Fig. 14.

Resolution. With the basic analysis indicated, the most important result as far as a mass spectrometer is concerned is the resolution of the device. Still treating a two dimensional problem with a rotating electric field, and assuming a collector for the resonant ions is located at a radius r_c from the origin, the resolution can be calculated as follows. Neglecting the jiggle motion of the particle and assuming $|\omega - \omega_c| \ll \omega_c$, the maximum radial excursion of a particle is

$$r_{max} = 2x_1 = 2qE/|\omega - \omega_c| m\omega \qquad \text{II-11}$$

If $\omega_c = qB/(m + \Delta m/2)$ and $\omega = qB/m$, then $r_{max} = mE/\omega_c B\Delta m$. Setting $r_{max} = r_c$, it follows that

$$m/\Delta m = r_c\omega_c B/4E = \pi N/2 \quad , \qquad \text{II-12}$$

where N is the number of revolutions the particle makes before hitting the collector ($N = r_c f_c B/E$) and Δm is the range of masses that would be collected. Equation II-12 states that the resolution ($m/\Delta m$) is directly proportional to the number of revolution a particle makes.

Another way to express the resolutioh is to find the range of frequency, $\Delta\omega$, over which a given mass particle would be collected. This result is

$$\Delta\omega = 4E/r_c B \quad \text{or} \quad \frac{\Delta\omega}{\omega_c} = \frac{4E}{r_c\omega_c B} = \frac{2}{\pi N} \quad . \qquad \text{II-13}$$

In the laboratory embodiment of the Omegatron, the electric field frequency is swept and collected current versus frequency displayed on an oscilloscope. Thus the frequency range over which an ion is collected is called the peak width, and $\Delta\omega$ measures this.

The important point here can be seen in equation II-12, where the resolution varies inversely with the electric field; thus high resolution is obtained simply by reducing the electric field - one of the big advantages of the Omegatron.

Ion energy. A resonant ion travels an average spiral path with the electric field always accelerating it. When it reaches the collector it has gained some energy. This energy can easily be calculated. When the ion is a radial distance r_c out, its velocity is $v = r_c\omega_c$ and so its kinetic energy is

$$KE = mv^2/2 = m(r_c\omega_c)^2/2 \quad . \qquad \text{II-14}$$

For a mass 18 ion with $r_c = 1$ cm and $\omega_c = 1.9\times10^6$ rad/sec , this gives KE = 34 e-v.

Clearly the energies involved in the Omegatron problem are all small enough so that relativistic effects can be completely neglected.

Path length. A resonant ion which spirals out to a collector at r_c travels an average distance πr_c per turn (neglecting jiggles), so the total path length traveled, L , becomes

$$L = \pi r_c N \quad . \qquad \text{II-15}$$

The significance of this length, other than that it becomes fairly long with high resolution, is in terms of possible gas scattering of the ions. The molecular mean free path in air at a pressure of 10^{-6} mm of Hg. is

something like 65 meters, so for $r_c = 1$ cm this would limit N to about 2100, at which point scattering would become significant. The corresponding resolution is one part in 3200. Thus even at such a background pressure no difficulty from gas scattering should be expected until extremely high resolution is required.

Jiggle motion. To show that the jiggle motion is indeed small and can be neglected, refer to Fig. 10 where the size of the jiggle is twice the radius of the cylinder generating the cycloid. This gives the jiggle a size of $2v/\omega_c = 2E/B\omega_c = r_c/\pi N = r_c \Delta m/2m$. Thus the jiggle size in proportion to the collector distance equals $\Delta m/2m$, and for any reasonable resolution, say one part in 100, this makes the jiggles negligible.

The effect of the counter rotating field necessary to describe the fixed direction, sinusoidally time-varying electric field case can be readily calculated and leads to jiggles comparable in size to those above, thus also negligible.

Initial velocities. The effect of x or y directed initial velocities on the ion trajectories can be easily seen. Referring to the coordinate system rotating at the electric field frequency, for a resonant ion an initial velocity would simply change the cycloid to a prolate or curtate trochoid. For an off resonance ion an initial velocity would simply change the epi- or hypocycloid to an epi- or hypotrochoid (may be either prolate or curtate depending on the direction of the initial velocity). The net effect is then just a change in the size and shape of the jiggle motion.

The size of the additional jiggle motion from an initial velocity can be estimated. Initial velocities arise primarily from the thermal

velocity of a gas molecule before it is ionized. Assuming the gas is in thermal equilibrium at room temperature, the root-mean-square velocity in the x-y plane is $v = \sqrt{2kT/m}$. For a mass 18 ion in only a magnetic field (3500 gauss), such a velocity would put the ion in a circular orbit of diameter 2.7×10^{-2} cm. The complete solution to the problem with initial conditions can now be obtained by adding this circular motion to the solution for the problem with zero initial conditions. But this extra jiggle motion is again a negligible amount and means that x-y initial velocities may be neglected.

Initial velocities in the z direction cause an ion to drift out of the measuring region and so decrease the number of collected ions (peak height). This effect will be considered later under the particular subject of peak height.

Space charge. A uniform space charge (of magnitude ρ) would produce a radial force on an ion a distance r from the origin of amount

$$F_r = \frac{q\rho}{2\epsilon_o} r \quad . \qquad \text{II-16}$$

This looks just like a radial spring from the origin of spring constant $K' = -q\rho/2\epsilon_o$. Referring the motion to a coordinate system rotating at half cyclotron frequency, the equation of motion for this case, from II-7, becomes

$$\begin{aligned} m\bar{a}_r &= -m\omega_c^2\bar{r} + q\bar{E} + (q\rho/2\epsilon_o)\bar{r} \\ &= (q\rho/2\epsilon_o - m\omega_c^2/4)\bar{r} + q\bar{E} \quad . \end{aligned} \qquad \text{II-17}$$

Thus the motion is identical (except ω_s has changed) with that of an ion with the same mass and charge but moving in a reduced magnetic field.

The only interesting effect of the uniform space charge is then to change the resonant frequency of an ion. The actual resonant frequency, ω_r , for small ρ , is

$$\omega_r = \frac{\omega_c}{2} + \sqrt{\frac{\omega_c^2}{4} - \frac{q\rho}{2\epsilon_o m}} \cong \omega_c \left(1 - \frac{q\rho}{2\epsilon_o B\omega_c}\right) \quad . \qquad \text{II-18}$$

For a mass 18 ion in a 3500 gauss field with $\rho = 10^{-8}$ coul/m^3, this gives a 0.1% lowering of the resonant frequency.

The more interesting space charge case, though, is when the space charge has a non-uniform distribution, particularly when it is crowded up around the origin. In this case the radial force is non-linear, as is the whole problem.

Nonlinearities. When the space charge has a non-uniform distribution that is still cylindrically symmetrical, a graphical method can be developed for finding the average trajectory of an ion. Actually this method can be applied to any cylindrically symmetrical, nonlinear effect; thus it can be used, for example, for finding average ion trajectories when the magnetic field has a radial variation in intensity. In the experimental Omegatron, the pole tips are very large and so it is reasonable to take the magnetic field as uniform, but a non-uniform space charge (in particular, a line charge) is still of interest. Again considering the case of an ion in a rotating applied electric field and referring the motion to a coordinate system rotating at the electric field frequency, the equation of motion from II-8 becomes

$$m\bar{a}_r = q(\bar{v}_r \times \bar{B}_1 + \bar{E}) - K\bar{r} + \bar{F}_r \quad , \qquad \text{II-19}$$

where $\bar{B}_1 = \bar{B}(1 - 2\omega/\omega_c)$ and $K = m\omega(\omega_c - \omega)$ and F_r is the radial force (which also may be any function of r) caused by any space charge. For example, if the space charge is simply a line charge at the origin of magnitude σ, then

$$\bar{F}_r = \frac{\sigma q}{2\pi \epsilon_o r^2} \bar{r} \quad . \qquad \text{II-20}$$

Eq. (17) may be rewritten for this case as

$$m\bar{a}_r = q(\bar{v}_r \times \bar{B}_1 + \bar{E}) - K'\bar{r} \qquad \text{II-21}$$

where $K' = K - F_r/r$ and thus K' varies to absorb the variations in F_r/r.

The important point now is that we are looking only for the average motion, and are not at all interested in the small jiggles. In the constant K' case, the average motion is obtained by drawing a circle through the origin whose center is at $x_r = x_1 = qE/K'$, as in Fig. 15. This is because, as we have already seen, a particle in a uniform magnetic field under the action of a radial spring from the origin and with zero initial velocity will travel an hypocycloid (epi- if K' is negative), while if the initial velocity is non-zero the path will be a hypotrochoid (again epi- if K' is negative), both of which give an average circular path centered at the origin with additional small jiggles.

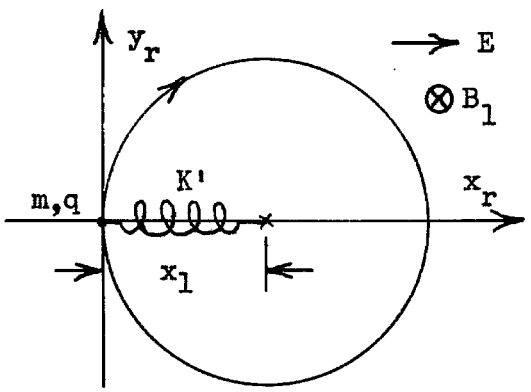

Fig. 15. Constant K' case.

If F_r/r varies with radius, then K' will vary also. In this case x_1 will vary as the particle moves and changes its radius. The path can be plotted graphically by connecting segments of circles centered at various x_1's which are calculated using the radial distance of the particle from the origin over each segment. This is a convenient graphical procedure for it involves only the use of a compass.

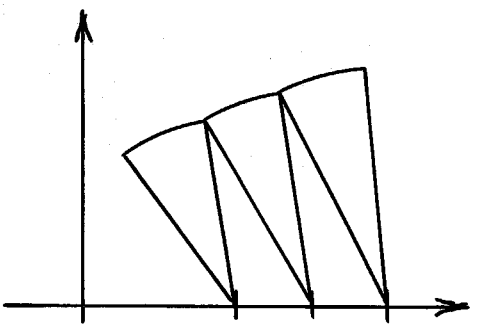

Fig. 16. Graphical construction.

When the space charge is in the form of a line charge of size σ located at the origin, the circular arcs center at

$$x_r = x_1 = \frac{qE}{m}\left[\omega(\omega_c - \omega) - \frac{q\sigma}{2\pi\epsilon_o m\, r^2}\right]^{-1} . \qquad \text{II-22}$$

For the purpose of plotting the results, it is convenient to normalize the variables. Linear dimensions can be normalized by scaling by the factor $(\omega_c B/E)$, thus let $u = (\omega_c B/E)x$ and $v = (\omega_c B/E)y$. Frequency can be expressed in terms of the percentage difference from resonance, $\delta = (\omega - \omega_c)/\omega_c$. In terms of the new variables, II-22 becomes

$$u_1 = x_1(\omega_c B/E) = \frac{-1}{(1+\delta)\delta + s_o^2/s^2} \qquad \text{II-23}$$

where $s = (\omega_c B/E)r$ and $s_o^2 = (\omega_c B/E)(\sigma/2\pi\epsilon_o E)$.

Of course an ideal line charge is not realistic for it would mean an infinite force on an ion at the origin. The actual space charge would probably be rather uniformly distributed in a small region near

the origin. This can be taken care of, for a uniform charge distribution of radius r_a, by centering the circular arc at

$$u_a = \frac{-1}{(1+\delta)\delta + s_o^2/s_a^2} \qquad \text{where} \quad s_a = r_a(\omega_c B/E) , \qquad \text{II-24}$$

when the ion is within r_a of the origin, and otherwise using the previous formula. The results of such a graphical procedure for several typical cases are shown in Figs. 17-21 in terms of the normalized variables.

Fig. 17 shows, for reference, the ion trajectories with no space charge. Fig. 18 shows the ion trajectories for the particular case of $s_o^2 = 10$ and $s_a = 20$. For the typical operating conditions cited earlier ($B = 3500$ gauss, $E = 50$ volts/m, $\omega_c = 1.9 \times 10^6$ rad/sec), these numbers correspond to a line charge $\sigma = 2.1 \times 10^{-12}$ coul/m and an $r_a = 0.15$ cm (approximately 1/16"). Fig. 19 shows the trajectories for $s_o^2 = 10$ and $s_a = 10$. Fig. 20 and 21 show them for $s_o^2 = 50$, $s_a = 30$ and $s_o^2 = 50$, $s_a = 20$, respectively. Clearly the concentration of charge near the origin decreases the maximum radial excursion of the particle. It also has the effect of lowering the apparent resonant frequency and narrowing the peak width.

The general conclusion to be drawn from the non-linear ion trajectories is that there exists a maximum radial excursion for all ions. Physically this results from the fact that the effective resonant frequency of an ion varies with radius, so that an ion which must start in resonance to get out at all soon becomes out of resonance and spirals back in. Generally, the maximum radial excursion decreases with electric field so that as the electric field is reduced in an

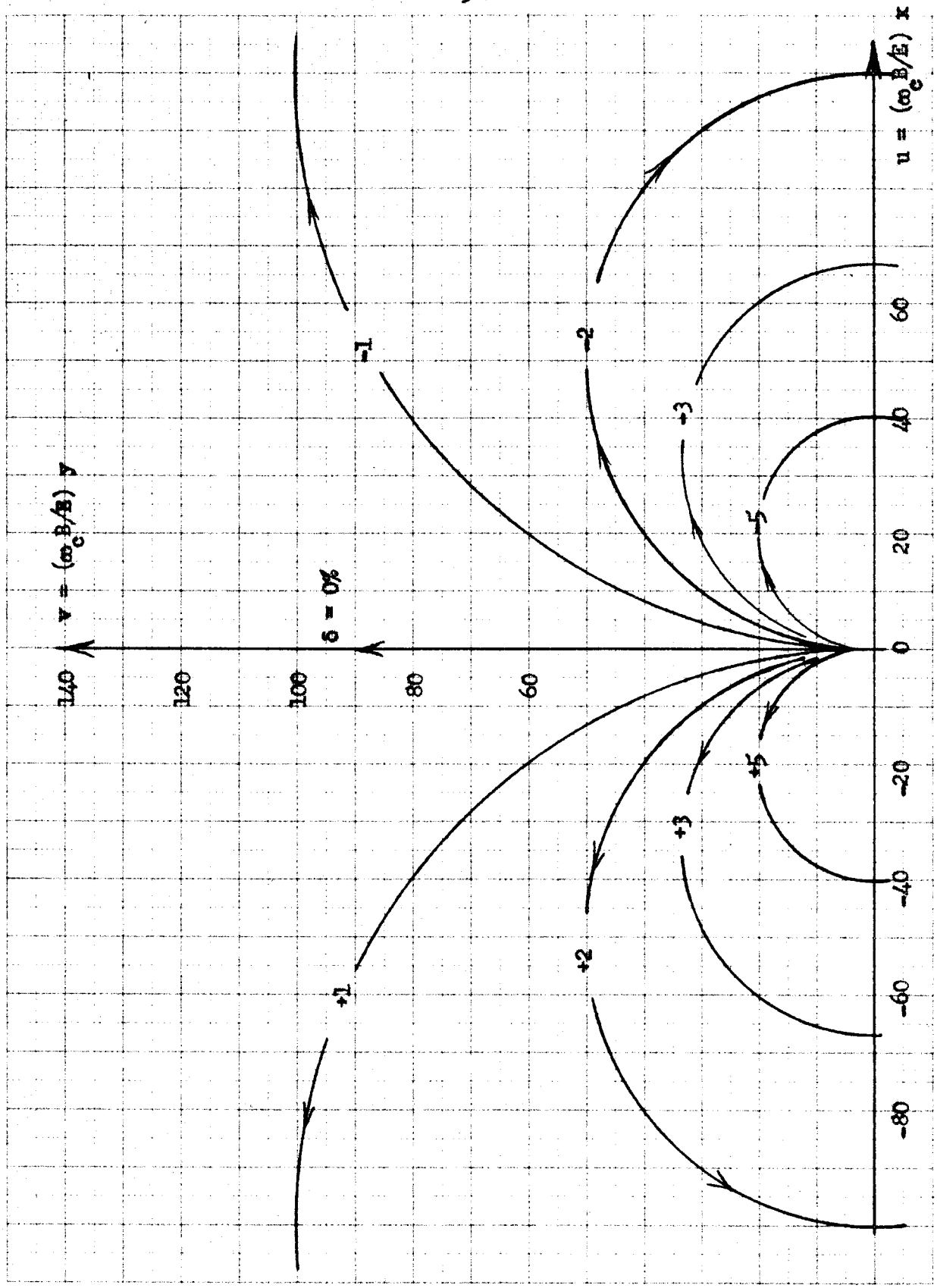

Fig. 17. No space charge.

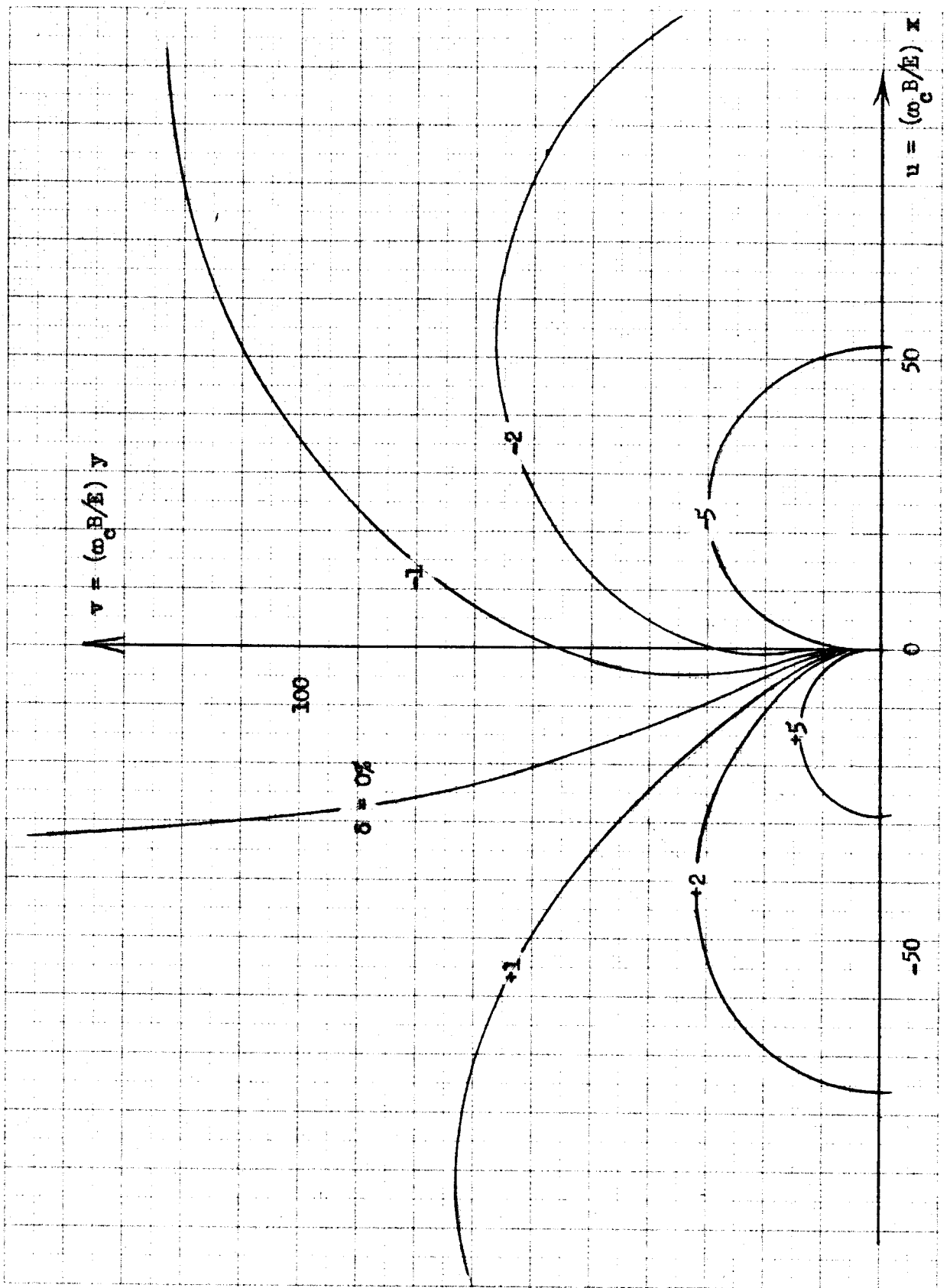

Fig. 18. $s_o^2 = 10$ and $s_a = 20$.

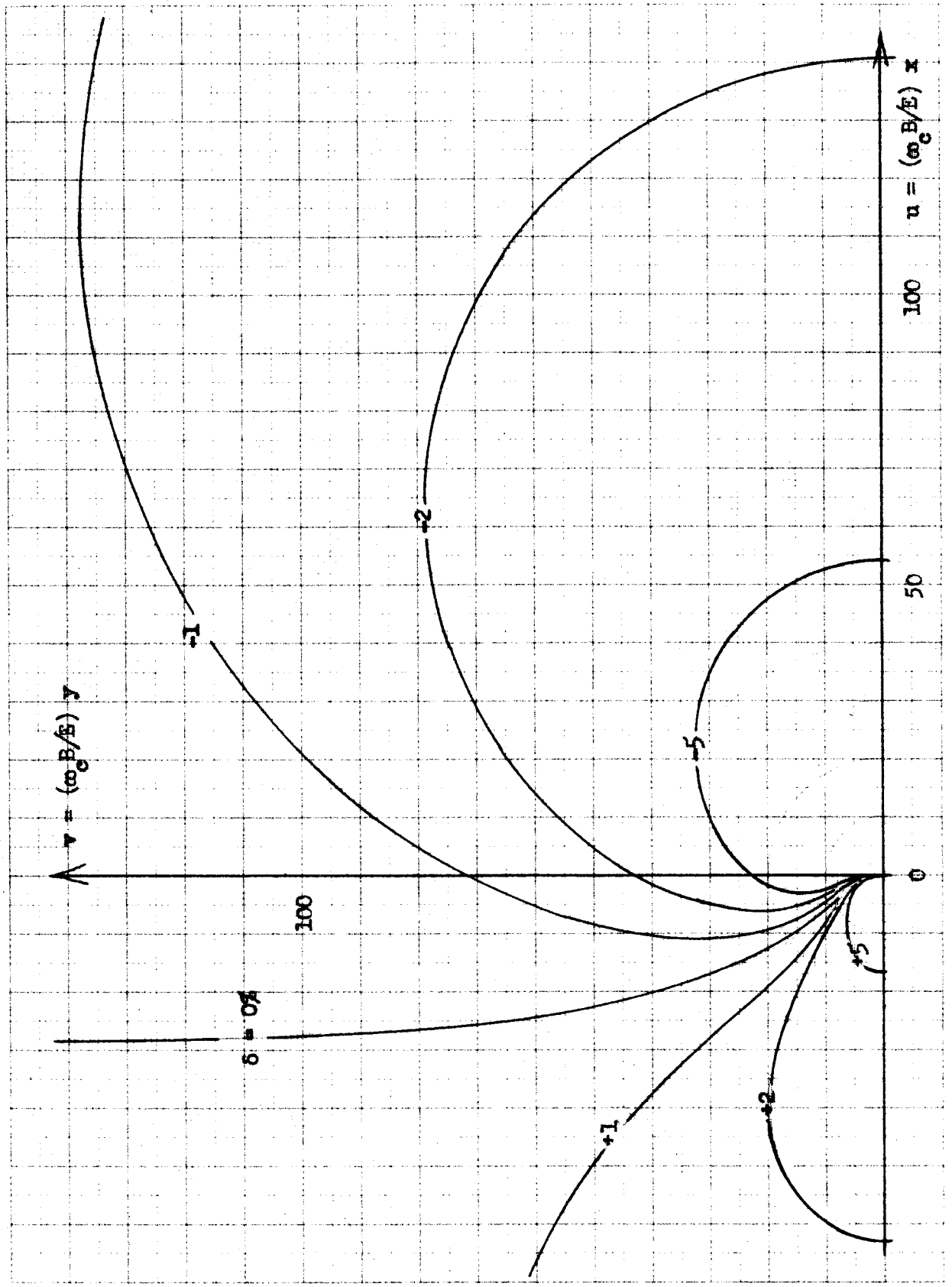

Fig. 19. $s_o^2 = 10$ and $s_a = 10$.

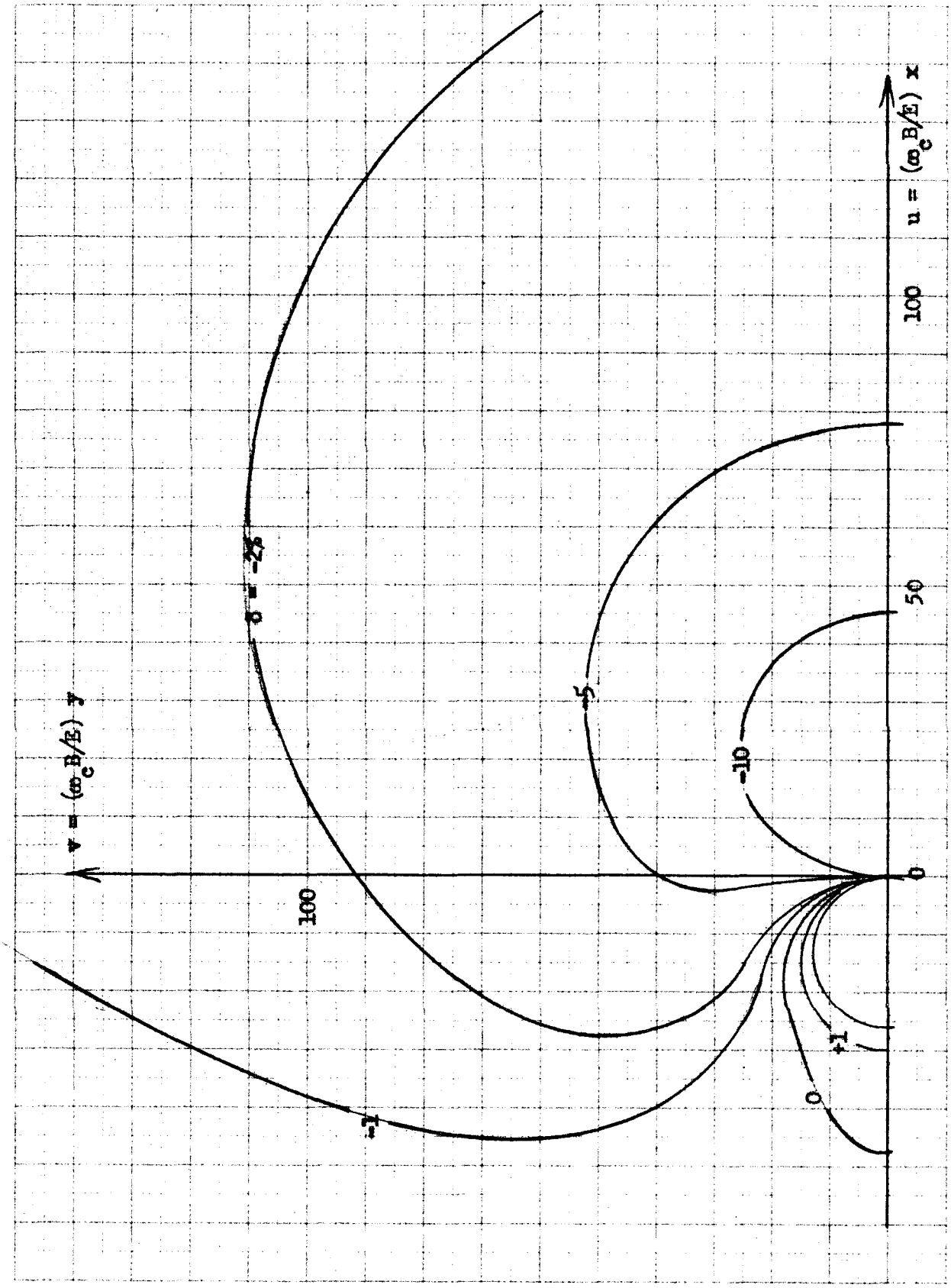

Fig. 20. $s_o^2 = 50$ and $s_a = 30$.

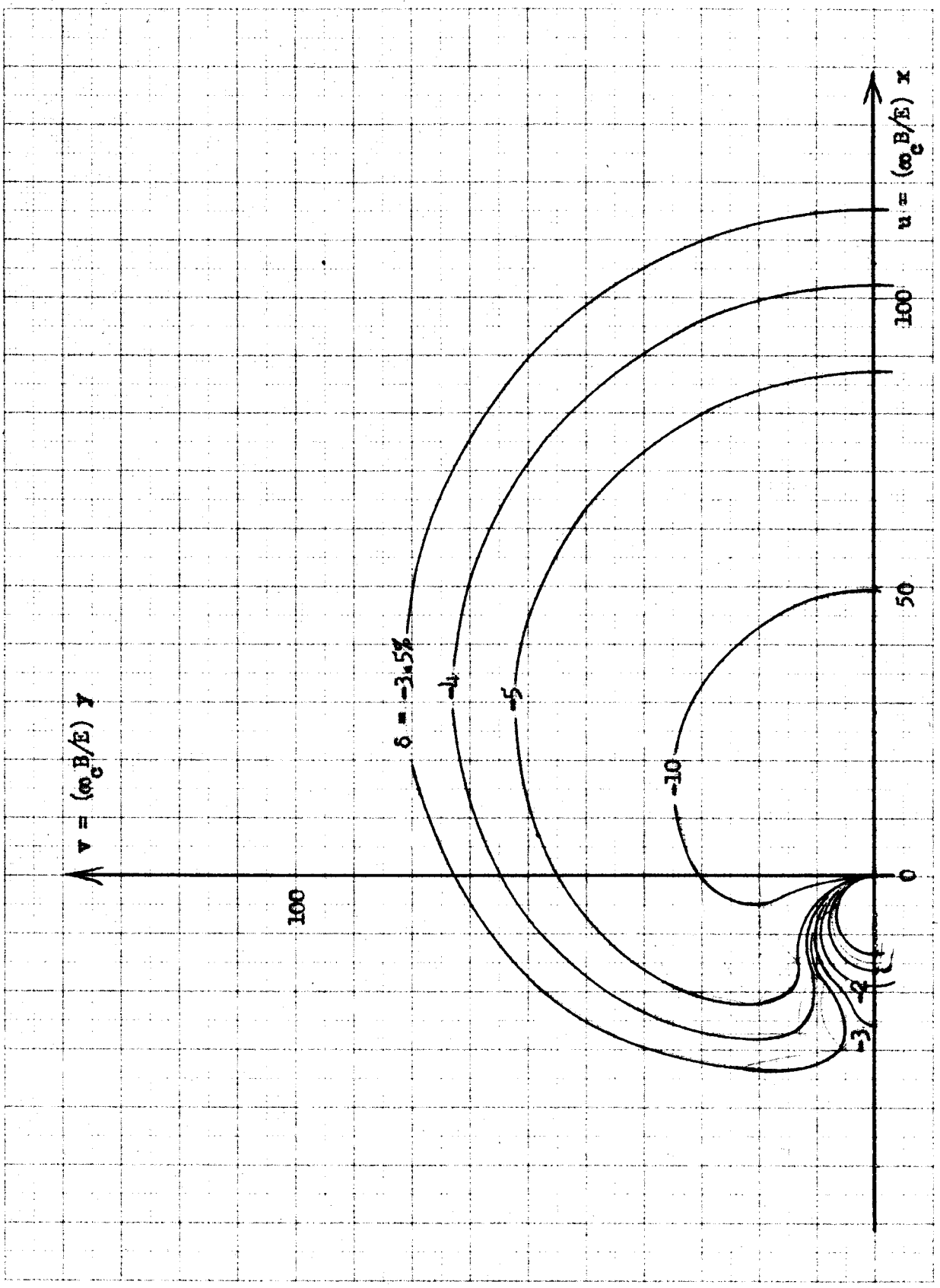

Fig. 21. $s_o^2 = 50$ and $s_a = 20$.

attempt to get more resolution, a point is reached where no more ions are collected. This then clearly limits the ultimate resolution of the Omegatron and appears to be a very serious difficulty.

Electric field fringing. The actual Omegatron is essentially a cube of equipotential surfaces, two sides of which form the electric field plates. The other four sides are generally maintained at some small DC potential to aid in trapping the ions. This three-dimensional character causes the electric field to fringe quite badly rather than to be uniform as has been assumed. To investigate effects from fringing of the electric field, the field pattern must be calculated. The actual potential distribution inside a cube of side a may be easily calculated. Considering the top and bottom ($x = +a/2$ and $x = -a/2$) to be at $+V_o/2$ and $-V_o/2$ respectively and the other four sides to be at ground; a solution of Laplace's equation gives

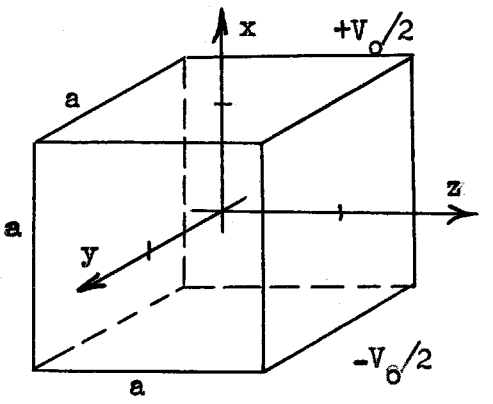

Fig. 22.

$$V/V_o = \sum_{m,n} B_{mn} \cos m\pi z'/2 \cos n\pi y'/2 \sinh \beta_{mn} x' , \qquad \text{II-25}$$

where $m = 1,3,5 \cdots$, $n = 1,3,5 \cdots$, $x' = 2x/a$, $y' = 2y/a$,

$z' = 2z/a$,

$$\beta_{mn} = \frac{1}{2}\sqrt{m^2 + n^2} ,$$

and $$B_{mn} = \frac{8(-1)^{(m+n-2)/2}}{mn\pi^2 \sinh \beta_{mn}} .$$

A different form for the potential which has better convergence at the

top and bottom plates may be found by first subtracting out a uniform electric field. Then

$$V/V_o = x'/2 + \sum_{m,n} B'_{mn} \sin m\pi x'/2 \left[\cos n\pi y'/2 \cosh \beta_{mn} z' + \cos n\pi z'/2 \cosh \beta_{mn} y'\right] , \qquad \text{II-26}$$

where $m = 0,2,4, \cdots$, $n = 1,3,5, \cdots$

and $$B'_{mn} = \frac{8(-1)^{(m+n-1)/2}}{m n \pi^2 \cosh \beta_{mn}} .$$

From these potentials the vertical electric field along the axis $(y = z = 0)$ may be calculated $(E'_x = E_x a/V_o)$ as

$$-E'_x = 1 - 0.291 \cos \pi x' + 0.0145 \cos 2\pi x' - \cdots \qquad \text{II-27}$$

while along the z axis (or y axis by symmetry)

$$-E'_x = 0.755 \cos \pi z'/2 - 0.0345 \cos 3\pi z'/2 + 0.0015 \cos 5\pi z'/2 - \cdots \qquad \text{II-28}$$

Using these expressions the equipotentials and flux lines may be plotted in the x-z plane $(y = 0)$ and in a parallel plane at $y' = 1/2$, and these plots are shown in Fig. 23. It is quite clear that E_x, the desired component, does not vary too badly except quite near the sides of the cube.

The horizontal electric field has a rather mixed behavior, but near the origin of the coordinate system it can be roughly approximated by the first term in its series. This gives

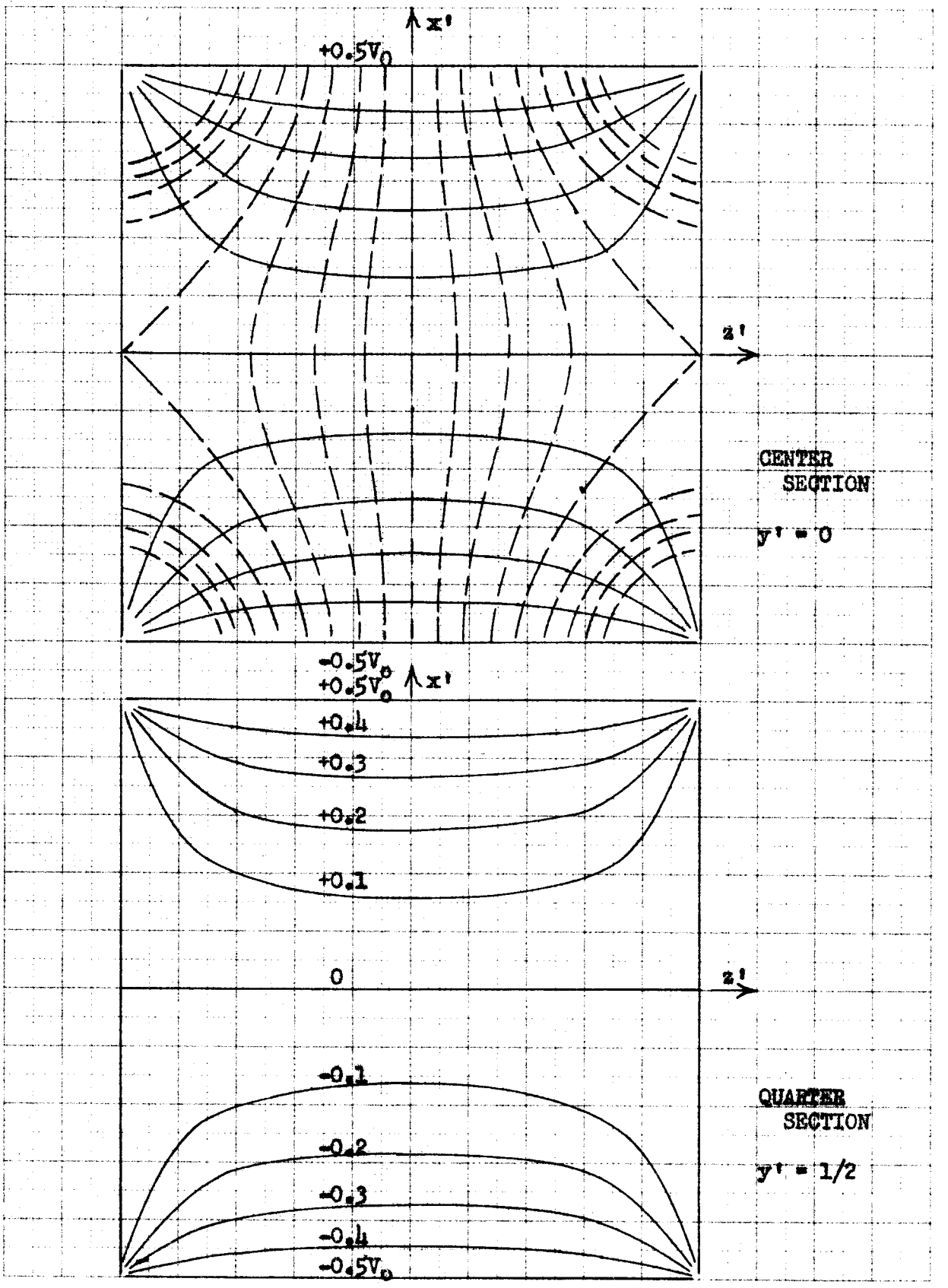

Fig. 23. Equipotentials and flux lines.

$$E'_z = 0.56 \sin \pi z'/2 \cos \pi y'/2 \sinh 2.22 x' \qquad \text{II-29}$$

where $E'_z = E_z a/V_o$ and the next largest term in the series is of the order of 0.03. Furthermore, near the origin the sine and sinh may be approximated by their arguments, giving

$$E'_z = 2 x'z' \qquad \text{or} \qquad E_z = 8 xz V_o/a^3 \ . \qquad \text{II-30}$$

Trapping is usually applied through a positive voltage connected to the two plates at $z = +a/2$ and $z = -a/2$, so the potential and field distribution under these conditions is also of interest. Taking the trapping voltage to be V_t and the other four plates to be at ground, the potential inside the cube is

$$\frac{V}{V_t} = \sum_{m,n} A_{mn} \cos \frac{m\pi x'}{2} \cos \frac{n\pi y'}{2} \cosh \alpha_{mn} z' \ , \qquad \text{II-31}$$

where $\alpha_{mn} = \frac{\pi}{2}\sqrt{m^2 + n^2}$ and $A_{mn} = \frac{16(-1)^{m+n-2/2}}{\pi^2 mn \cosh \alpha_{mn}}$.

At the center of the cube this gives $V = 0.199\ V_t$. The vertical electric field along the x axis ($y = z = 0$) can be calculated from the above potential as

$$E'_x = 1.072 \sin \frac{\pi}{2} x' - 0.066 \sin \frac{3\pi}{2} x' + 0.003 \sin \frac{5\pi}{2} x' + \cdots .$$

At the top plate this gives $E_x = 1.156\ V_t/a$. The horizontal electric field E_z at the center of a side plate ($x = y = 0$, $z = a/2$) is just twice the E_x at the top, $E_z = -2.3\ V_t/a$. This follows by superimposing on the problem just solved a similar problem with the plates at $y = \pm a/2$ raised in potential to V_t and then the vertical

field at the top is the same as E_z at the side in the original problem.

Z-instability. A resonant ion travels essentially in a circular path (actually a spiral) 90^o out of phase with the electric field. As far as the ion's z motion is concerned, E_z from the fringing RF electric field looks like a restraining spring from the origin whose spring constant varies with time from both V_o's variation and the variation in x. For motion near the origin, the restraining force can be written

$$F_z = qE_z = (8qV_o/a^3)\, xz$$

where $$V_o = V_{max} \cos \omega_c t \ .$$

If the ion is on a circular path of radius r and in resonance, $x = r \sin \omega_c t$ so that

$$F_z = (4qV_{max}\, r/a^3)(\sin 2\omega_c t)\, z \ .$$

The equation of motion for the ion in the z direction only becomes

$$m\ddot{z} + F_z + F_z' = 0$$

where F_z' is any additional time-independent z force (from trapping, for example) and will be taken of the form kz. Then

$$d^2z/dt^2 + \left[(4qV_{max}r/ma^3) \sin 2\omega_c t + k/m\right] z = 0 \ . \qquad \text{II-32}$$

Letting $2\omega_c t = \tau$, $qV_{max}r/\omega_c^2\, ma^3 = \epsilon$ and $k/4\omega_c^2 m = \delta$ this becomes

$$d^2z/d\tau^2 + (\epsilon \sin\tau + \delta)\, z = 0 \ . \qquad \text{II-33}$$

This is the form of the Mathieu equation (31) for which the stability

regions are known. Numerically, for the typical case of a mass 18 ion with V_{max} = 1 volt , a = 1 inch, $\omega_c = 1.9 \times 10^6$ rad/sec and r = a/4 , the constant defined above has the value $\epsilon = 6.5 \times 10^{-4}$. This very small value of ϵ in the Mathieu equation essentially guarantees stability for all positive values of δ .

A resonant ion which is off center in the z direction still sees a spring from the origin whose spring constant varies sinusoidally, but if the z motion of the ion is small this can best be treated as a sinusoidal applied force in the z direction. To show that the z motion of an ion is indeed small, an estimate can be made. For $z' = \frac{1}{2}$ and r = a/4 the maximum E_z is, from II-29

$$(E_z)_{max} = 0.2\ V_{max}/a \quad .$$

With this as the only driving force on a mass 18 ion, and other conditions as above, the sinusoidal excursion of the ion has a peak value of roughly 1×10^{-3} inches, a size which is clearly negligible.

Electric field fringing, x-y effect. Fringing of the electric field also means that in the x-y plane the field is not uniform, so splitting it into two counter rotating components does not completely describe it. The total electric field could be described by two rotating components plus a small extra field. This small extra field would vary both in time and in direction as far as a particular ion is concerned. Considering the results of the preceding section, it seems pretty clear that the effect of this small extra field would be to add more jiggle motion to the ion but still of a negligible amount. When a resonant ion is fairly far out, this extra field has a component along

the ion path in the forward direction; it therefore appears to somewhat strengthen the forward rotating electric field. The total amount of this strengthening can be estimated (from Fig. 23) as something like 10% to 20% at most and so is of no great concern here.

Ionization. In traveling through the spectrometer proper, some of the electrons in the electron beam collide with molecules of the gas and form ions. What happens to these ions (those not in resonance) and the electrons knocked off is of great importance in the operation of the device. Because of the very strong magnetic field, all the electrons remain very close to the original beam (a 45 e-v electron travels a circle of radius 0.002 inches in 3500 gauss). Likewise, the non-resonant ions also remain quite close to the beam (typically within about 0.02 inches). Therefore the real problem is almost a one-dimensional one and the only way electrons and ions can escape is out the ends of the beam.

The standard ionization rate(11) for a 67 volt electron beam is about 20 ions per electron per centimeter of path for a gas pressure of 1 mm of Hg. Under normal operation the background gas pressure is 2×10^{-6} mm of Hg. and the electron current 0.05 μamp, so for a path length of one inch the total ion production corresponds to an ion current of 5×10^{-12} amps (assuming single ionization).

The standard assumptions for low pressure gaseous conduction (32, 33,34) are:

(a) The ions move without interaction under the forces of any electric fields present. They have Maxwellian initial velocities with a temperature essentially that of the gas.

(b) The electrons move with a great deal of interaction and thus their density follows Boltzman's law,

$$\rho = \rho_o \exp(eV/kT_e) , \qquad \text{II-34}$$

where ρ is the electron charge density, e is the charge on an electron, k is Boltzman's constant, and T_e is the equivalent temperature of the electron gas. The electrons have a Maxwellian velocity distribution of zero mean at a temperature corresponding to 1 to 10 e-v of energy.

There are generally two electrons produced per ion; one is the incident electron (which loses most of its energy) while the other is the electron knocked off the atom in ionizing it. The electrons have a high energy because the incident electron's energy is high and not all of its energy is used in ionization. The ions have a low energy because in an electron-ion collision the large mass ratio means that very little kinetic energy is transferred.

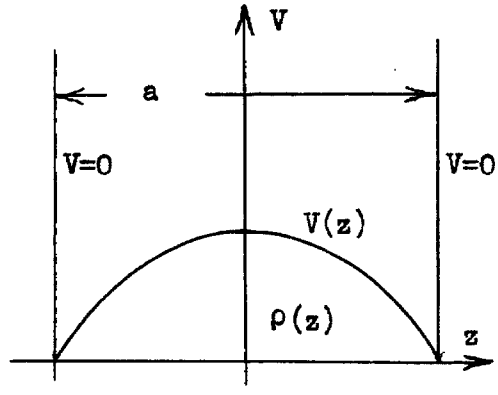

Fig. 24.

As a simple approximation to the real problem, consider two plates at zero potential between which non-interacting ions are being produced uniformly in space and time at a rate J_i (charge per unit volume and time) with zero initial velocity, and ask what is the steady state potential and charge distribution. This neglects the electrons and ion initial velocities, and makes a one-dimensional problem. If ρ is the charge density, one of Maxwell's equations,

$(\rho = \nabla \cdot \bar{D})$ gives

$$\rho(z) = - \epsilon_o \, d^2V/dx^2 \ , \qquad \text{II-35}$$

while conservation of charge gives

$$\rho(z) = \int_0^z (J_i/v) \, dz' = J_i \sqrt{m/2q} \int_0^z \frac{dz'}{\sqrt{V(z') - V(z)}} \ . \qquad \text{II-36}$$

A solution for $V(z)$ which satisfies both II-35 and II-36 is $V(z) = A - Cz^2$. If this is substitutèd into II-35 and II-36, for equality C must be

$$C = (J_i \, \pi/4\epsilon_o)^{2/3} \, (m/2q)^{1/3} \ . \qquad \text{II-37}$$

Thus $\qquad V(z) = C\left[(a/2)^2 - z^2\right] \quad$ and $\quad \rho(z) = 2\epsilon_o C \ . \qquad$ II-38

To get a feel for the numbers, consider this simplified problem to apply over just the area of the electron beam in the omegatron. Take the beam diameter as 1/16" and length 1" with a total ion current of 10^{-12} amps of mass 18 ions. J_i becomes 6.2×10^{-5} amp/m^3 while $V(0) = 0.124$ volts and $\rho = 1.41 \times 10^{-7}$ coul/m^3 . Again using the beam area, this ρ is equivalent to a line charge of $\sigma = 0.9 \times 10^{-13}$ coul/m .

To show that the electrons really are negligible in this problem, assume $kT_e = 1$ e-v (a rather pessimistic value), then, from II-34

$$\rho_e = \rho_{el} \exp(eV/kT_e) \ , \qquad \text{II-39}$$

where ρ_{el} is the electron space charge density at the edge. At the center, $\rho_{eo} = 1.13 \, \rho_{el}$ and the electron density is practically

constant. At the edge electrons escape because of their velocity component normal to the wall, and the number of electrons escaping (expressed as current density) is

$$i_e = \rho_{el}\sqrt{kT_e/2\pi m_e} \quad , \qquad \text{II-40}$$

where m_e is the electron's mass. By conservation of charge, this must be equal to the number of electrons produced, so set $i_e = 2J_i a$ where a is the length of the electron beam. Then

$$\rho_{el} = 2J_i a \sqrt{2\pi m_e/kT_e} \quad . \qquad \text{II-41}$$

Using the same numbers as before this gives $\rho_{el} = 1.28 \times 10^{-11}$ coul/m^3 a factor of 10^4 smaller than the ion charge density and clearly negligible.

Neglecting the ion initial velocities is justified simply in terms of the potential--the ions have initial energies of about 0.0248 e-v, while in traveling from the center to the edge they gain 0.124 e-v. Their initial velocities would have a small effect on the potential distribution at the center, but this can be neglected.

The simplified one-dimensional problem just solved is really too simple to adequately describe the Omegatron because the magnetic field confines the ions and electrons to remain essentially along the electron beam. Thus the problem is strictly a two-dimensional one. Of course one could solve exactly the problem of a circular pencil of space charge in a conducting cube, but such a solution would be much more complicated than the results justify. A good approximation to the complete solution can be obtained by assuming a uniform pencil-shaped distribution of ion

charge and a parabolic potential distribution along the axis of the pencil. The coefficients for the parabolic potential and the size of the ion charge are obtained by finding the exact electric field at the end of the pencil and its associated charge. Near the end of the pencil the rest of the cube may be neglected (beam diameter small compared with the cube size), so the problem may be treated as a beam ending on an infinite conducting surface. The conducting surface may then be replaced by the image of the beam and the electric field on the axis of the beam written as

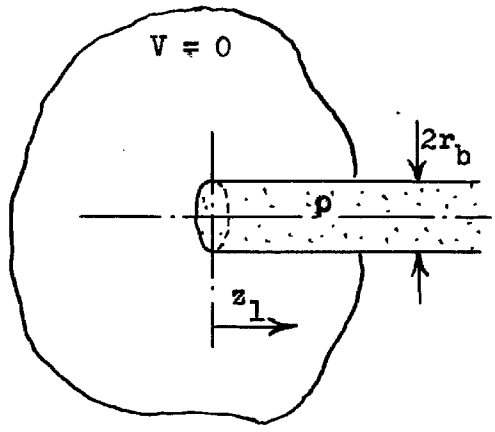

Fig. 25

$$E(z_1) = 2\int_0^{z_1} dz_1 \int_0^{r_b} dr \; \frac{\rho z_1 2\pi r}{4\pi \epsilon_o (r^2 + z_1^2)^{3/2}}$$

$$= (\rho/\epsilon_o)\left[\sqrt{z_1^2 + r_b^2} - z_1\right] \quad . \qquad \text{II-42}$$

In terms of an equivalent line charge σ, $E(z_1 = 0) = \sigma/r_b \pi \epsilon_o$. Assuming a parabolic potential, $V(z) = C_1(a^2/4 - z^2)$ where $z = z_1 + a/2$, at the edge $E(z = a/2) = C_1 a$. Equating these two E's fixes C_1 as

$$C_1 = \sigma/a\, r_b \pi \epsilon_o \quad . \qquad \text{II-43}$$

As in the case of uniform overall ion production, conservation of charge gives (neglecting any radial potential variation)

$$\sigma = \int_0^z \frac{I_i \, dz'}{a\sqrt{2q/m}\sqrt{V(z') - V(z)}} \qquad \text{II-44}$$

where I_i is the total ion production expressed as current. Thus

$$\sigma = (I_i/a)(\pi/2)\sqrt{m/2qC_1}$$

and so $C_1 = (I_i/2a^2 r_b \epsilon_o)^{2/3} (m/2q)^{1/3}$ and $\sigma = \pi(I_i^2 \epsilon_o m r_b/8aq)^{1/3}$. II-45

For a numerical value, same conditions as before, $\sigma = 6 \times 10^{-15}$ coul/m and $V(0) = 1.7 \times 10^{-3}$ volts. This is clearly too small a line charge to cause any serious difficulties.

When a trapping voltage is applied the story is quite different. Trapping causes an inward directed electric field at the ends of the beam and the ion space charge must build up enough to cancel this field plus an additional amount as in Eq. II-45 to force the ions out. If the trapping produces a field E_t at the ends, the ion charge density to cancel this, from II-43 , is

$$\sigma_i = \epsilon_o \pi r_b E_t \quad . \qquad \text{II-46}$$

One volt of trapping produces a field of about 50 volts/m , so with this trapping $\sigma = 1.1 \times 10^{-12}$ coul/m . This is definitely large enough to cause nonlinear trajectories--see Fig. 19--and would mean the applied RF would have to be of the order of a volt or more for ions to be collected at all. This space charge effect is a very serious one and appears to be the crux of the Omegatron's difficulties.

Peak Height. The maximum ion current collected as the frequency is swept over resonance for a particular ion is called the peak height. The largest factor affecting the peak height is the z drift of the ions due to their thermal velocities. Assuming there is no trapping field, that ions are produced uniformly along the length a of the electron beam with a Maxwellian distribution of velocities (of non-zero mean for generality) in the z direction and that the collector is at a radial distance r_c and of length a (not exact, but a good approximation), the number of ions collected n , as a percentage of the number produced N , can be found. In order to reach the collector, those ions with a z-directed velocity v must come from a length $(a - \tau|v|)$ of the electron beam, where τ is the transit time of an ion. Thus

$$n = \int_{-a/\tau}^{a/\tau} \frac{N(1 - \tau|v|/a)}{\sqrt{2\pi}\, v_m} \; e^{-(v - v_o)^2} \, dv \qquad \text{II-47}$$

where v_m is the root-mean-square ion velocity about the mean and v_o is the average velocity. In a normal thermal ion at temperature T , $v_o = 0$ and $v_m = \sqrt{kT/m}$. Carrying out the integral

$$\frac{n}{N} = \frac{1}{2}\left[\operatorname{erf}(s+b) + \operatorname{erf}(s-b)\right] + \left(\frac{b}{2s}\right)\left[\operatorname{erf}(s+b) - \operatorname{erf}(s-b) - 2\operatorname{erf}(b)\right] \qquad \text{II-48}$$

$$+ \left(\frac{1}{2} s\sqrt{\pi}\right)\left[e^{-(s-b)^2} + e^{-(s+b)^2} - 2e^{-b^2}\right]$$

where $s = a/\sqrt{2}\,\tau\, v_m$, $b = v_o/\sqrt{2}\, v_m$ and erf is the error function (Dw. 590). A resonant ion has an average radial velocity (neglecting the jiggle motion) $v_r = E/B$, so its transit time $\tau = r_c/v_r = r_c\, B/E$ and thus

$$s = E(a/\sqrt{2}\, r_c B v_m) \ . \qquad \text{II-49}$$

With $b = 0$, II-48 reduces to the result given by C.E. Berry (35) in an article explaining some of the effects of ion initial velocities on a normal 180° spectrometer.

Numerically, for a mass 18 ion under the typical conditions used before and at room temperature, $s = 0.5$. Equation II-48 is shown plotted in Fig. 27 for various values of b .

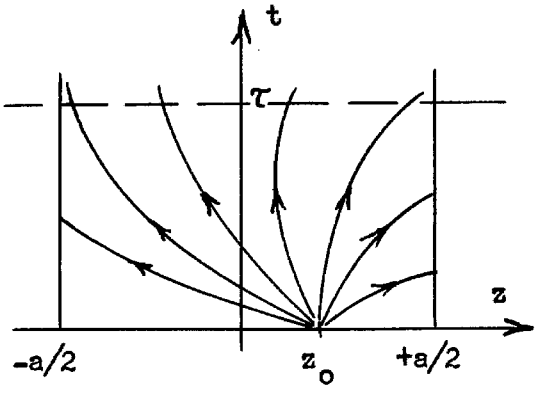

Fig. 26.

It is somewhat interesting to speculate on what the effect of a z-directed electric field would be on peak height. Consider ions which start at $z = z_o$ with a Maxwellian velocity distribution of zero mean and ask for the range of initial z directed velocities over which an ion will reach the collector at time τ . An ion will reach the collector only if its z coordinate is never greater than $+a/2$ or less than $-a/2$, otherwise it will strike the side of the spectrometer and disappear. The conditions on its initial velocity such that $|z_{max}| \leq a/2$ are:

For $0 \leq \tau \leq \sqrt{2a/g}$

$v_o \leq v \leq v_2$ for $-a/2 < z_o \leq z_1$

$v_1 \leq v \leq v_2$ for $z_1 \leq z_o \leq a/2$

For $\sqrt{2a/g} \leq \tau \leq 2\sqrt{2a/g}$

$v_o \leq v \leq v_2$ and $z_2 \leq z_o \leq a/2$

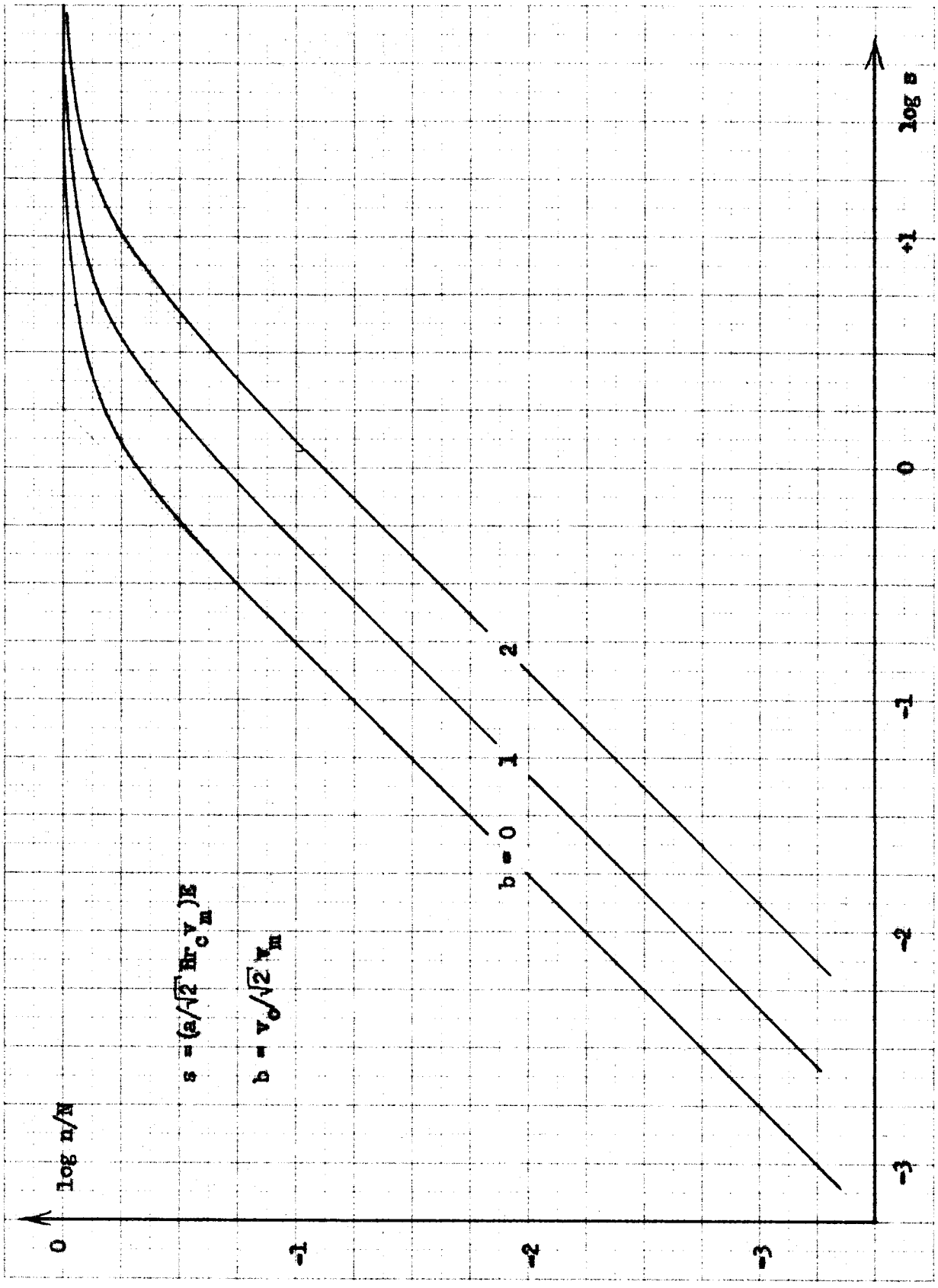

Fig. 27. Peak height, thermal z drift.

where $v_o = -\sqrt{g(a+2z_o)}$, $v_1 = -a/2\tau - z_o/\tau - a\tau/2$,

$v_2 = a/2\tau - z_o/\tau - a\tau/2$, $g = qE_z/m$,

$z_1 = g\tau^2/2 - a/2$, $z_2 = g(\tau - \sqrt{2a/g})^2/2 - a/2$.

For $\tau \geqslant 2\sqrt{2a/g}$, no ions reach the collector. In terms of these conditions, the percentage number of ions reaching the collector may be written

For $0 \leqslant \tau \leqslant \sqrt{2a/g}$

$$\frac{n}{N} = \int_{-a/2}^{z_1} \frac{dz_o}{a} \int_{v_o}^{v_1} f_o(v)\, dv + \int_{z_1}^{a/2} \frac{dz_o}{a} \int_{v_1}^{v_2} f_o(v)\, dv \qquad \text{II-50}$$

For $\sqrt{2a/g} \leqslant \tau \leqslant 2\sqrt{2a/g}$

$$\frac{n}{N} = \int_{z_2}^{a/2} dz_o/a \int_{v_o}^{v_2} f_o(v)\, dv \qquad \text{II-51}$$

where $f_o(v)$ is the Maxwellian distribution of zero mean,

$$f_o(v) = (1/\sqrt{2\pi}\, v_m) \exp(-v^2/2v_m^2) .$$

The solution of these integrals, though rather tedious in algebra, is straightforward and gives

for $0 \leqslant \tau \leqslant \sqrt{2a/g}$

$$\frac{n}{N} = (\tfrac{1}{2}s)\Big[(s - c/s)\,\mathrm{erf}(s - c/s) - (c/s + s/8c)\,\mathrm{erf}(2c/s) - (c/s)\,\mathrm{erf}(c/s) + (s + c/s)\,\mathrm{erf}(s + c/s) + 1/\sqrt{\pi}\Big[e^{-(s - c/s)^2} - e^{-(c/s)^2} - (\tfrac{1}{2})\, e^{-(2c/s)^2} + e^{-(s + c/s)^2}\Big]\Big] \qquad \text{II-52}$$

while for $\sqrt{2a/g} \leqslant \tau \leqslant 2\sqrt{2a/g}$

$$\frac{n}{N} = \left(\frac{1}{2}s\right)\Big[(c/s - s + s/8c)\ \mathrm{erf}(2c/s - 2c) - (c/s)\ \mathrm{erf}(c/s)$$
$$+ s(1 - 1/8c)\ \mathrm{erf}(2\sqrt{c}) + 1/\sqrt{\pi}\Big[(1/2)(1 + s/\sqrt{c})\ e^{-4(c/s - c)^2} \qquad \text{II-53}$$
$$- e^{-(c/s)^2} + (s/2\sqrt{c})\ e^{4c}\Big]\Big]$$

where $s = a/\sqrt{2}\,\tau\, v_m$ and $c = ga/4v_m^2$. These results are shown plotted in Fig. 28 for various values of c .

The conclusions from Fig. 27 are that, as was to be expected, thermal z drift would cause the peak height to drop as the electric field is decreased. Thus in an attempt to get higher resolution with a smaller electric field, a point will be reached where not enough ions reach the collector. This then will limit the resolution of the device, but with only thermal (of zero or non-zero mean) initial velocities, the peak height drops proportionally to the RF for small RF so the resolution can always be extended by increasing the sensitivity of the electrometer. On the other hand, if there is an external E_z the peak height drops more rapidly with RF (see Fig. 28) and for any particular E_z there exists a minimum RF below which no ions are collected. In this latter case, nothing short of canceling the E_z would allow the resolution to be extended. This could be a very serious difficulty if it were not for the fact that any stray E_z could very easily be canceled by applying an external voltage to the Z plates.

The electric field from the space charge is outward on both sides of the cube of the Omegatron so can't be canceled by an average E_z , but from the calculated size of that electric field (see section of ionization) it would not be a significant effect. And of course ordinary trapping would offset it.

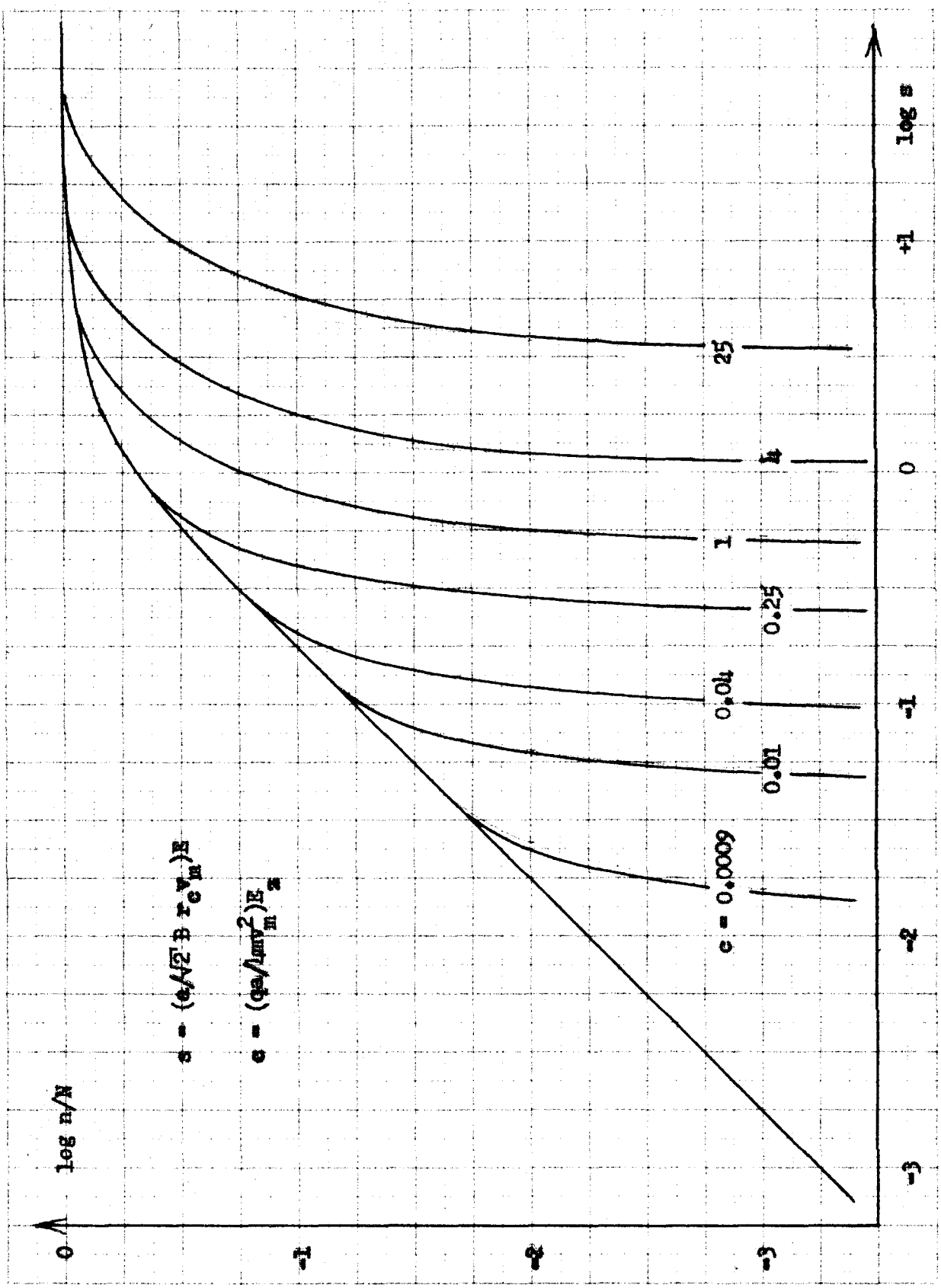

Fig. 28. Peak height, external field.

Peak shape. Under ideal conditions, without any z fields or space charge effects, the peak shape is perfectly rectangular. All ions of a given mass either travel far enough out to be collected or they do not, and the width of the peak, neglecting any jiggle motions, has already been calculated in II-13. If the z drift of the ions is now included, the corners of the peak become slightly rounded. This is because an ion reaching the collector when the frequency is slightly off resonance requires a slightly longer time--in the rotating coordinate system it travels the arc of a circle rather than a straight line--and more of them drift out before being collected. Actually the maximum transit time is a factor of $\pi/2$ greater than the resonant transit time (circumference of a semi-circle compared to its diameter). This rounding has its worst effect when the RF is small (see Fig. 27) for then the percentage number of ions collected at the peak edge compared to the peak center is smallest, and is in fact just inversely proportional to the transit time. This is indicated in Fig. 29 on an arbitrary logarithmic scale of collected ion current. From Fig. 29 it is clear that this effect is really a rather small one.

The jiggle motion which has so far been neglected, tends to spread out the ion trajectories (in the rotating coordinate system, see Fig. 14) into bands following the same average trajectory. From an exact solution of the rotating electric field case plus the effect of the counter rotating field and any electric field fringing, the jiggle motion produces a band of finite width (quite small under normal conditions). From the thermal initial velocities, the band is not exactly defined because a few ions have a very high initial velocity and thus a large

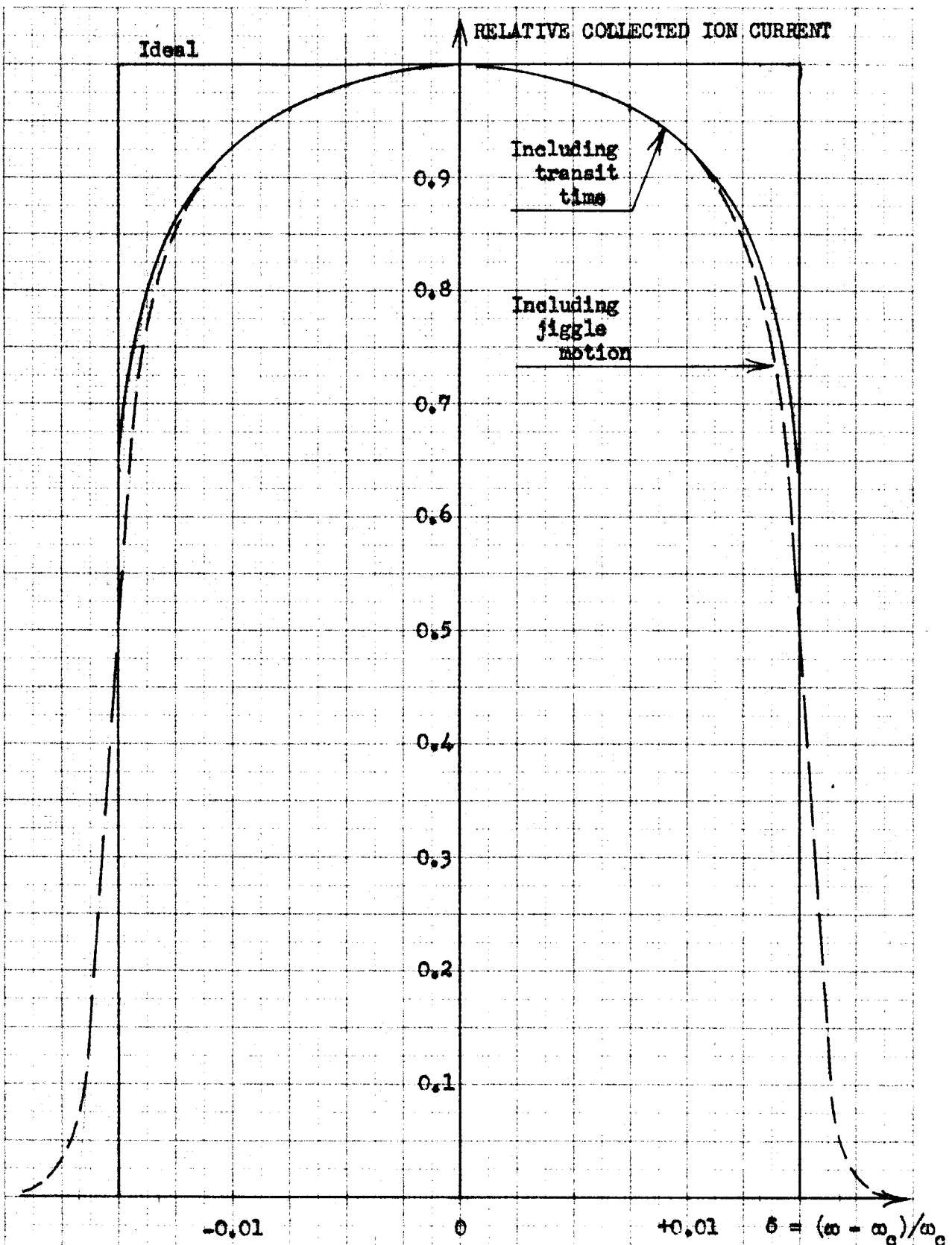

Fig. 29. Peak shape.

jiggle motion. The majority of the ions however have initial velocities about equal to the root-mean-square thermal velocity v_m and so the band has a sort of average width given by the corresponding jiggle. This has been calculated before (see section on initial velocities) and for typical conditions gives a jiggle width of about 0.03 cm. The bands in the ion trajectories, of course, mean that the peak shape is still more rounded and the sides of the peaks will be sloping. It is hardly worth while to calculate an exact peak shape for this condition, but an engineering guess as to the peak shape can be made and is included in Fig. 29.

A uniform space charge simply changes the center frequency of the peak, leaving the peak shape essentially as it was. A non-uniform space charge, and in particular a line charge, causes the peaks to become narrower. This can be seen in terms of Figs. 17-21, where the frequency range of ions that travel out a certain distance is narrower than that of the corresponding case of no space charge. The physical explanation of this is that the nonlinear forces from the space charge make the system behave somewhat like a narrow band filter. If the frequency is off a small amount from that which gets the ions farthest out, the ion trajectory is strongly confined. In addition to narrowing the peak width, a non-uniform space charge would make the peaks unsymmetrical. This can be seen, for example, in Fig. 21, where one must imagine

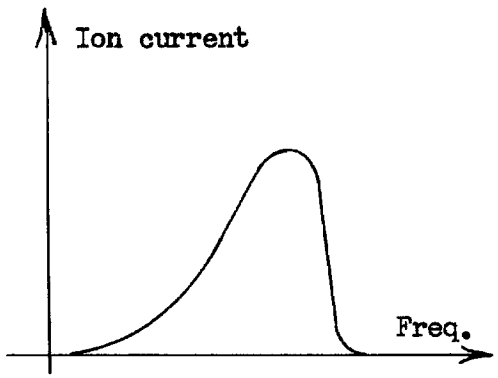

Fig. 30. Unsymmetrical Peak.

bands to account for the jiggle motion, replacing the lines in the trajectories. As the frequency is increased from below that for maximum excursion ($\delta = -3.5\%$), the collected ion current slowly increases, while above the frequency of maximum excursion the collected ion current decreases rapidly. Essentially this is because of the sudden change in radial excursion for ions above and below the frequency of largest excursion; that is, because of the unsymmetry in ion trajectories.

The unsymmetrical peak shape was noticed by Sommer, Hipple and Thomas in their work with the Omegatron (2), but unexplained. They also showed that they had some positive ion space charge, so in view of the latter the unsymmetrical peak shape can now be explained.

Peak frequency. Experimentally, one measures the frequency at which maximum ion current is collected and calls this the peak frequency. Several factors can make the measured frequency different from the theoretical cyclotron resonance frequency, qB/m . As has already been pointed out, a uniform positive space charge will simply lower the peak frequency, and given the amount of space charge, the change in frequency can be calculated through II-18 . A non-uniform space charge also lowers the frequency, but of course in a very non-linear way. Given the space charge in size and distribution, the frequency of maximum collected ion current can be calculated as outlined in the section on nonlinearities.

The last factor which influences the peak frequency is the fringing of the trapping field. For an ion spiraling in the center plane of the Omegatron a positive trapping voltage produces a radial field and thus a radial force on the ion. The effect of this radial

force is the same as an increase in the ion's mass (i.e., the same as an increase in its centrifugal force), and this in turn is equivalent to a decrease in its cyclotron resonance frequency. In the center plane of the Omegatron, the actual electric field from a positive trapping voltage is not quite radial because the Omegatron is a cube rather than a cylinder, but its deviation is small and can be neglected. This radial electric field varies almost linearly in proportion to the radius--actually, from the section on electric field fringing, its variation is more sinusoidal with radius than anything else because the first term in the series is the most important one, but the linear assumption is a pretty good one. The trapping field fringing thus affects an ion in exactly the same way as a uniform space charge, i.e., it leaves the ion trajectory unchanged but lowers the apparent resonant frequency. The size of this effect can easily be calculated in the same way as the uniform space charge effect was; in a coordinate system rotating at half cyclotron frequency the radial spring from the transformation plus the spring from the trapping are combined and the resonance for this new system determined. If the trapping voltage V_t produces an electric field $E_t = 1.156\ V_t/a$ at $y = z = 0$, $x = a/2$, the apparent spring constant is $K_t = 2qE_t/a$. Using this spring constant in II-7 leads to

$$\omega_r = \frac{\omega_c}{2} + \sqrt{\frac{\omega_c^2}{2} - \frac{K_t}{m}} \simeq \omega_c(1 - K_t/m\omega_c^2)$$

$$= \omega_c(1 - 2.3\ V_t/a^2 B\omega_c) \quad , \qquad \text{II-54}$$

where ω_r is the apparent resonant frequency. Thus one volt of trapping on a mass 18 ion under typical conditions gives a frequency shift of 1.2%.

CHAPTER III

EXPERIMENTAL RESULTS

Equipment. Much of the equipment associated with the operation of the Omegatron is rather standard laboratory test gear and so deserves only brief mention, but a few of the parts should be more completely described. The DC voltages for the various plates in the Omegatron were all obtained from batteries as indicated in the block diagram and potentiometers.

(1) Magnet. The magnet body was built by another experimenter for a different purpose but was modified for the Omegatron. It is a conventional type of electromagnet which under normal conditions is supplied by four six-volt batteries and draws 12 amps. Under these conditions it produces a magnetic field of about 3500 gauss in the gap. The pole tips are cylindrical, of mild steel and 6" in diameter with a gap spacing of 1.5". Because of their large diameter and the small size of the Omegatron proper, it is reasonable to neglect all fringing of the magnetic field and assume B is constant over the area of the Omegatron. Any inhomogeneities in the iron of the tips themselves would be expected to drop off in a distance of the order of the size of the inhomogeneity, and thus small flaws are not significant. There

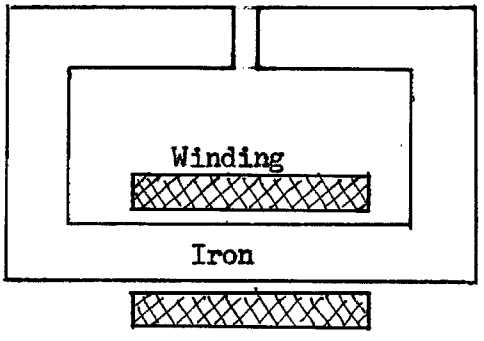

Fig. 31.

was no experimental evidence to indicate any large flaws. For the sake of completeness, a curve of gap flux density versus magnet current is included in Appendix II.

(2) Vacuum system. The vacuum system was also mostly the result of an earlier experimenter's work. The high vacuum is obtained from two all-glass mercury diffusion pumps operated in cascade. The diffusion pump nearest the fore pump has a convergent nozzle to give a large pressure drop while the second pump has a divergent nozzle for high pumping speed at low pressure. There is a liquid air trap in the line and then a glass-to-copper seal leading to the spectrometer proper. A standard ionization gauge (RCA 1949) is attached between the cold trap and the spectrometer.

There is a great advantage in using a mercury diffusion pump for experimental work on a mass spectrometer, and that is because mercury and its isotopes are well known and only mercury would contaminate the vacuum. With an oil diffusion pump there is some cracking of the oil in the pump from heating, and this gives a wide range of masses which might be found as background.

A gas handling system has been built for the Omegatron. Essentially it consists of a large flask into which the gas sample can be admitted at reduced pressure (about 0.1 mm of Hg.). Connecting the flask to the spectrometer proper is a capillary leak (a piece of capillary tubing drawn down to an inside diameter of 0.15 mm and of length 25 mm) which allows the gas to leak in at as high a rate as possible without spoiling the vacuum.

(3) RF system. In block diagram form, the RF system has already

been described (see Fig. 6). As indicated there, the output from a standard TV sweep generator (RCA FM Sweep Generator, Model WR-53A) is 8 to 10.5 MC and this is swept over a maximum range of 0.8 MC . The output from this oscillator is mixed in a standard mixer tube circuit with the output from a fixed frequency 10.5 MC oscillator. From the mixer the signal is amplified in a conventional one-tube wide band RC coupled amplifier, then passed through a split load phase inverter to two cathode follower output tubes. The output from these tubes goes directly to the RF plates of the Omegatron. RF amplitude control is obtained by varying the output from the FM sweep oscillator. The center frequency of the RF is varied by tuning the FM sweep oscillator.

The low sweep rate is actually obtained from the display oscilloscope (a DuMont 304A) using external capacitors to slow down its regular sweep rate. Since the FM sweep generator on "external sweep input" requires a push-pull signal, the sweep voltage from the oscilloscope is fed through a DC coupled phase inverter and a pair of cathode followers to the FM sweep generator. A gain control in the phase inverter allows the frequency range swept to be varied in width.

The circuits associated with the RF system are all quite standard radio circuits. A circuit diagram for them is included in Appendix III.

(4) Electrometer. The electrometer circuit used with the Omegatron is shown in block diagram form in Fig. 32. The block labeled -A is an amplifier of gain -A with a very high input impedance, a detailed circuit for which may be found in Appendix III. By standard circuit analysis,

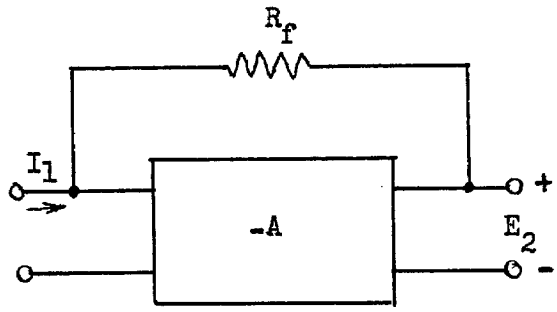

Fig. 32. Electrometer.

$$E_2 = \frac{-A\, R_f\, I_1}{1 + A} \qquad \text{III-1}$$

so that if a voltmeter is attached to the output it will read in proportion to the input current. For the Omegatron, $R_f = 10^{11}$ ohms, A is about 5,000, and the maximum deflection sensitivity of the oscilloscope used to read E_2 is about 0.1 volts for full scale, so this would correspond to a current sensitivity of 10^{-12} amps. Higher sensitivity can be obtained with the circuit of Fig. 33, where R_1 and R_2 form a voltage divider after E_2 for the feedback. The current sensitivity is increased inversely as the ratio of the voltage division (assuming $R_f > R_1$ or R_2) and a factor of 10 increase is easily obtained.

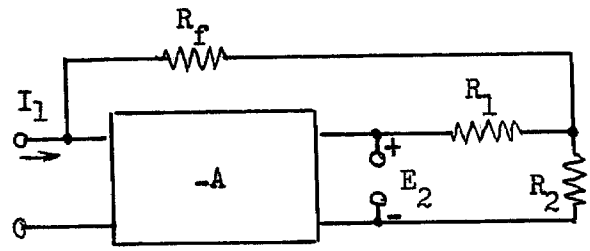

Fig. 33. More sensitive circuit.

Referring to Fig. 32, the input impedance is

$$Z_1 = \frac{E_1}{I_1} = \frac{R_f}{1 + A} \qquad \text{III-2}$$

which for a high gain amplifier is relatively small. This low input impedance combined with an output voltage proportional to input current makes an ideal ammeter, which is what is really wanted for the Omegatron. In addition, the low input impedance means that any stray resistance to ground at the input is less significant and any stray capacitance has less effect. In fact, a capacitance C_1 from the input to ground makes equation III-1 look like

$$\frac{E_2}{I_1} = -\frac{A}{1+A}\,\frac{1}{1+\tau_1 s} \qquad \text{III-3}$$

where $\tau_1 = R_f C_1/(1+A)$, and thus the time constant of the circuit is reduced by essentially the gain of the amplifier. The reduction of the time constant is really the biggest advantage of this circuit.

Johnson noise in the feedback resistor is the limiting factor in sensitivity. In the circuit of Fig. 32, such noise can be accounted for by inserting a noise voltage source E_n in series with R_f, where $\overline{E_n^2} = 4kT\,R_f\,\Delta f$. If the amplifier gain is very high, its input voltage is substantially zero and the output noise is just equal to the resistor noise. The root-mean-square noise in the output then increases in proportion to the square root of the resistance, while for a given current input the signal output increases directly as the resistance. Thus the signal to noise ratio increases in proportion to the square root of the resistance, the larger resistance the better. The limiting factor on the size of the resistance is when shot noise from the grid current becomes appreciable. Since the grid shot noise current is $\overline{I_{gn}^2} = 2e\,I_q\,\Delta f$, where I_q is the average grid current, the total mean-square output noise is

$$\overline{E_{2n}^2} = (4kT + 2e\,I_g\,R_f)\,R_f\,\Delta f\,. \qquad \text{III-4}$$

Therefore the two effects are equal when $R_f = 2kT/eI_g$, which for room temperature gives $R_f = 0.05/I_g$. The electrometer input tube is a Victoreen type 5800, which has an average grid current less than 10^{-15} amps. Thus Johnson noise and grid current noise are equal when $R = 5 \times 10^{13}$ ohms. Above this value, increasing R does not improve

the signal to noise ratio.

The input tube of course adds noise in the shot effect from its plate current, but this contribution is negligible. Tube noise may be treated by an equivalent voltage generator in series with the input grid, and the size of this generator calculated from the noise equivalent grid resistance for the tube. Since as far as noise is concerned the input is open circuited, a noise generator in series with the grid behaves just like the noise associated with the feedback resistance and so appears directly at the output. But since the noise equivalent grid resistor for most tubes is of the order of 10K to 100K ohms, and might be as bad as an order of magnitude greater for this particular input tube, it is still negligible compared with the Johnson noise from the feedback resistor.

Of course in the circuit of Fig. 33 the signal to noise ratio is unchanged by R_1 and R_2, so their effect is simply to increase the voltage level at the output. In normal operation at maximum sensitivity, R_1 and R_2 form a 10 to 1 voltage divider and so the RMS noise voltage at E_2 is $10\sqrt{4kTR_f \Delta f}$. With $R_f = 10^{11}$ ohms and at room temperature, this gives $4 \times 10^{-4} \Delta f$ volts/$\sqrt{\text{cps}}$. Maximum signal under these conditions is 0.1 volt, so for a signal to noise ratio of 100, Δf would have to be 6 cps. Thus between the electrometer amplifier and the recording device, there must be a low pass filter with a cut off about 6 cps. This means that the sweep frequency used must be small compared to 6 cps in order to have good detail in the oscilloscope pattern. The actual sweep frequency has been set at 1/5 cps.

The only other parasitic element which might be significant would be a distributed capacitance across the feedback resistor. And analysis of the circuit in Fig. 34 shows

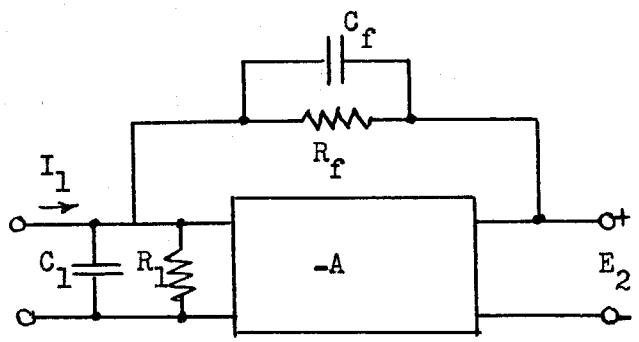

Fig. 34. Parasitic elements.

$$\frac{E_2}{I_1} = \frac{-A}{1+A} R_f \left[\left(1 + \frac{R_f}{(1+A)R_1}\right) + \left(C_f + \frac{C_1}{1+A}\right) R_f s \right]^{-1} . \qquad \text{III-5}$$

Thus C_f is significant only if large compared to $C_1/(1+A)$. One would expect C_f to be of the order of 0.1 uuf, being only the distributed capacity between the ends of the 10^{11} ohm feedback resistor, so $\tau_f = C_f R_f = 10^{-2}$ secs. and should cause no trouble.

Experimental results. For the main part, the experimental results agree with the theory as developed. Some spurious effects were noticed and exact reproducibility was not always obtainable. Generally this is explained by noting that the voltages involved in the Omegatron are all relatively small, of the order of one volt, while a small charge accumulation on the stainless steel plates if slightly dirty, could produce equivalent fields. Considerable effort was expended in an attempt to clean the conducting surfaces in the Omegatron, but such cleaning usually had a rather short life when it had any effect at all. Because of the nature of the system--soft solder connections and "O" ring seals--it was not possible to bake out the whole spectrometer in order to clean

the surfaces. Charging of slightly dirty metal plates is a common difficulty in mass spectrometers, and there is some evidence to indicate that such charging is more severe when the ions arrive at the metal surface nearly tangent, as many do in the Omegatron.

Peak Height. Most of the initial experimental results were obtained in terms of peak height because this is very easy to measure in the experimental setup. The mass 18 peak was generally used because it was prominent and appeared quite reliable. Fig. 35 is quite typical and shows peak height on a logarithmic scale (log I_c , where I_c is the collected ion current) plotted as a function of RF for various trapping voltages. Several things are clear from the figure:

(a) Peak height drops much more rapidly than linearly with RF for small RF voltages. This strongly suggests space charge difficulties. A DC z-directed field could also explain this difficulty, but an applied field did not correct it so it is ruled out.

(b) With no trapping, the minimum RF for a useful peak is so high that resolution is not very good.

(c) Trapping generally increases the size of the peak, but even at best there is a minimum RF for reasonable peaks. And for this to be a very low value of RF, a great deal of trapping is required.

(d) Some anomalous behavior occurs with high trapping. This is called peak splitting and will be discussed later.

Similar results have been found for hydrogen (mass 2), carbon monoxide (mass 28), oxygen (mass 32) and carbon dioxide (mass 44).

Peak Width. Generally, width of the peaks agrees pretty well with calculated values. The shape of the peaks was more rounded than the simple theory would predict, but the differences were estimated

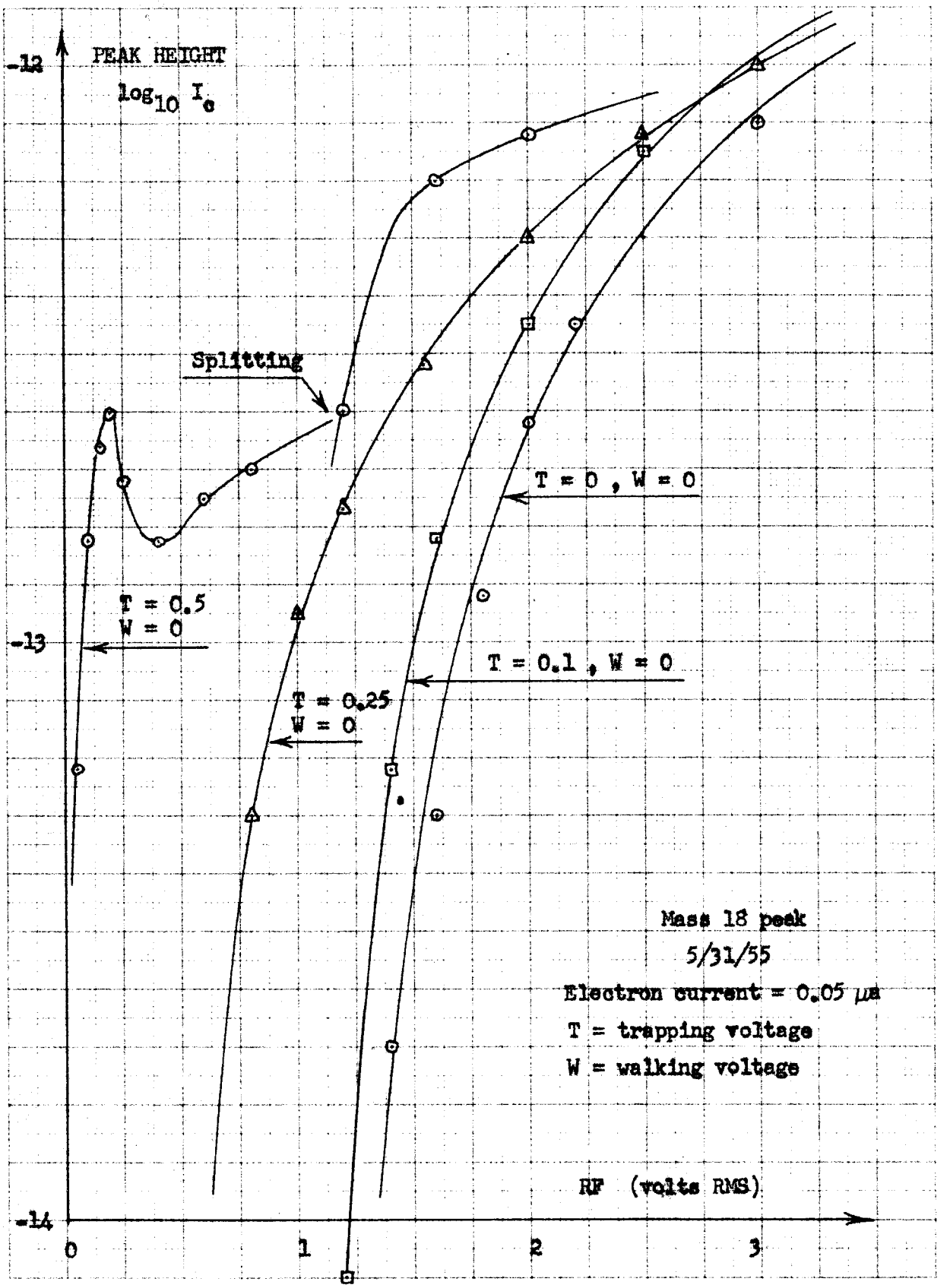

Fig. 35. Peak height versus RF.

to be reasonable in terms of including the effect of the various jiggle motions. Fig. 36 shows the mass 16, 17, 18 and 19 peaks run at RF = 3 volts (sensitivity here is 10^{-14} amps/div). Using equation II-13 for the theoretical peak width, one gets $\Delta\omega/\omega_c = 0.05$. This agrees qualitatively with the figure, the actual peaks being a little sharper. Resolution can be increased by lowering the RF, but in order to maintain peak size it is then necessary to use trapping. Fig. 37 shows mass 17, 18, and 19 at RF = 0.1 with a trapping of 0.35 volts. Resolution is clearly improved considerably, in fact more than is shown in the figure. The low pass filter suppressing the Johnson noise in the electrometer has widened the peaks somewhat. This can be seen in Fig. 38 where the horizontal scale has been expanded by a factor of four to show just the mass 18 peak. The triple peak appearing here is probably a form of peak splitting (discussed later) because a small amount of walking (0.05 volts) clears it up completely and leaves a very nice shaped mass 18 peak as shown in Fig. 39.

Another example of the high resolution obtainable with high trapping is shown in Fig. 40, where the mass 17 and 18 peaks are shown for RF = 0.4, trapping = 0.8 and walking = 0.3 volts. The small wiggles between the peaks are not real but just a momentary surge of noise. The non-symmetrical peak is also unreal, being caused by the low pass filter in the electrometer. This is demonstrated in Fig. 41 where the horizontal scale has been expanded by a factor of five to show the mass 18 peak itself in detail.

It is interesting to note that quite high resolution can be obtained even with the experimental Omegatron. It was possible to

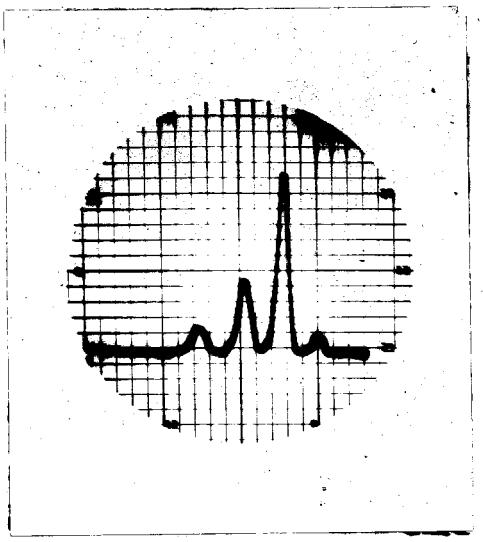

Fig. 36.

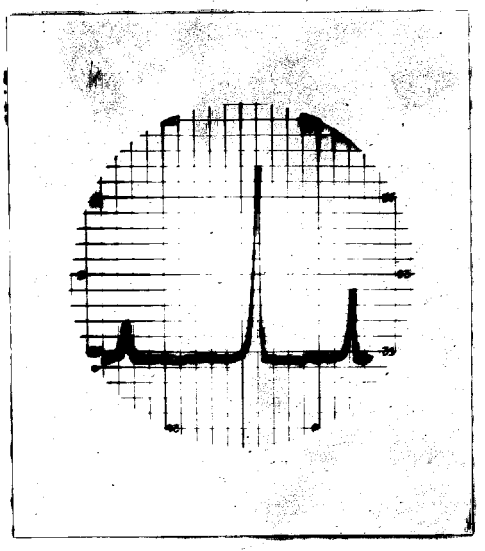

Fig. 37.

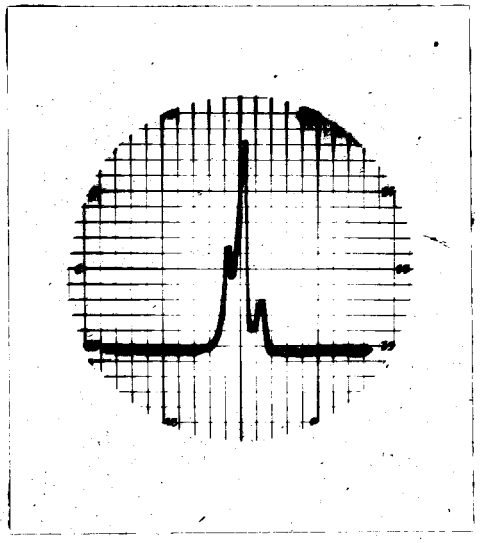

Fig. 38.

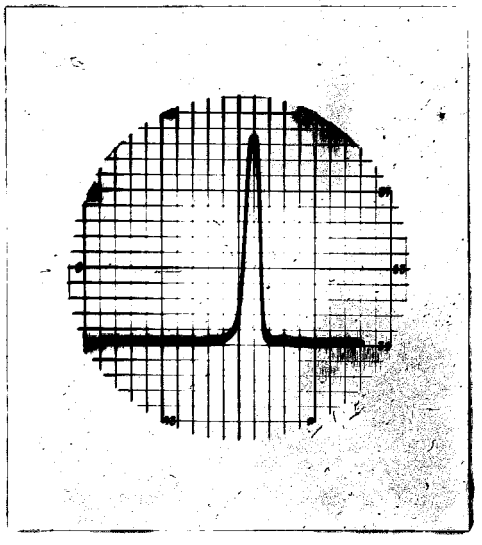

Fig. 39.

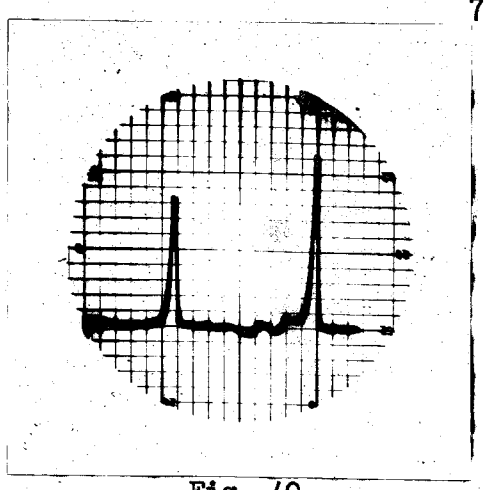

Fig. 40.

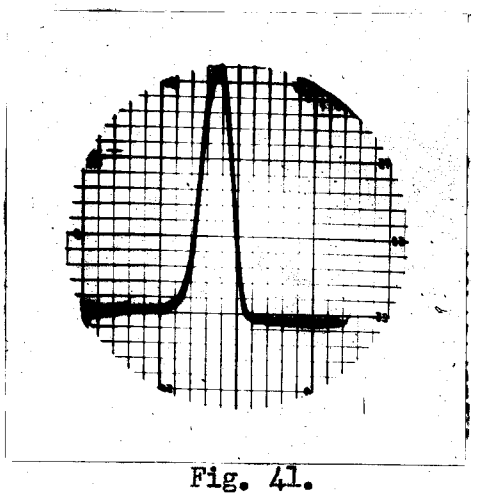

Fig. 41.

separate O_{16} and methane, CH_4, into two separate peaks by properly adjusting the Omegatron. Since the two masses differ by one part in 450, the resolution was estimated at something like one part in 1500. This high resolution could not be maintained at the higher masses, and even at mass 32 the resolution had dropped below one part in 500.

Fig. 42 shows peak width versus RF for several different masses. The significant point here is that although there is considerable scatter in the points the width is frequently narrower than the simple theory would predict. The only explanation of this seems to be in terms of space charge, which has been shown to have a sharpening effect on peaks.

Peak Frequency. Fig. 43 shows a typical plot of peak frequency as a function of trapping. For small values of trapping there is pronounced anomalous behavior and peak splitting, but above 0.4 volts trapping the behavior is quite uniform. The slope of the trapping versus frequency curve is just about twice the value that could be explained in terms of the trapping field fringing alone; presumably

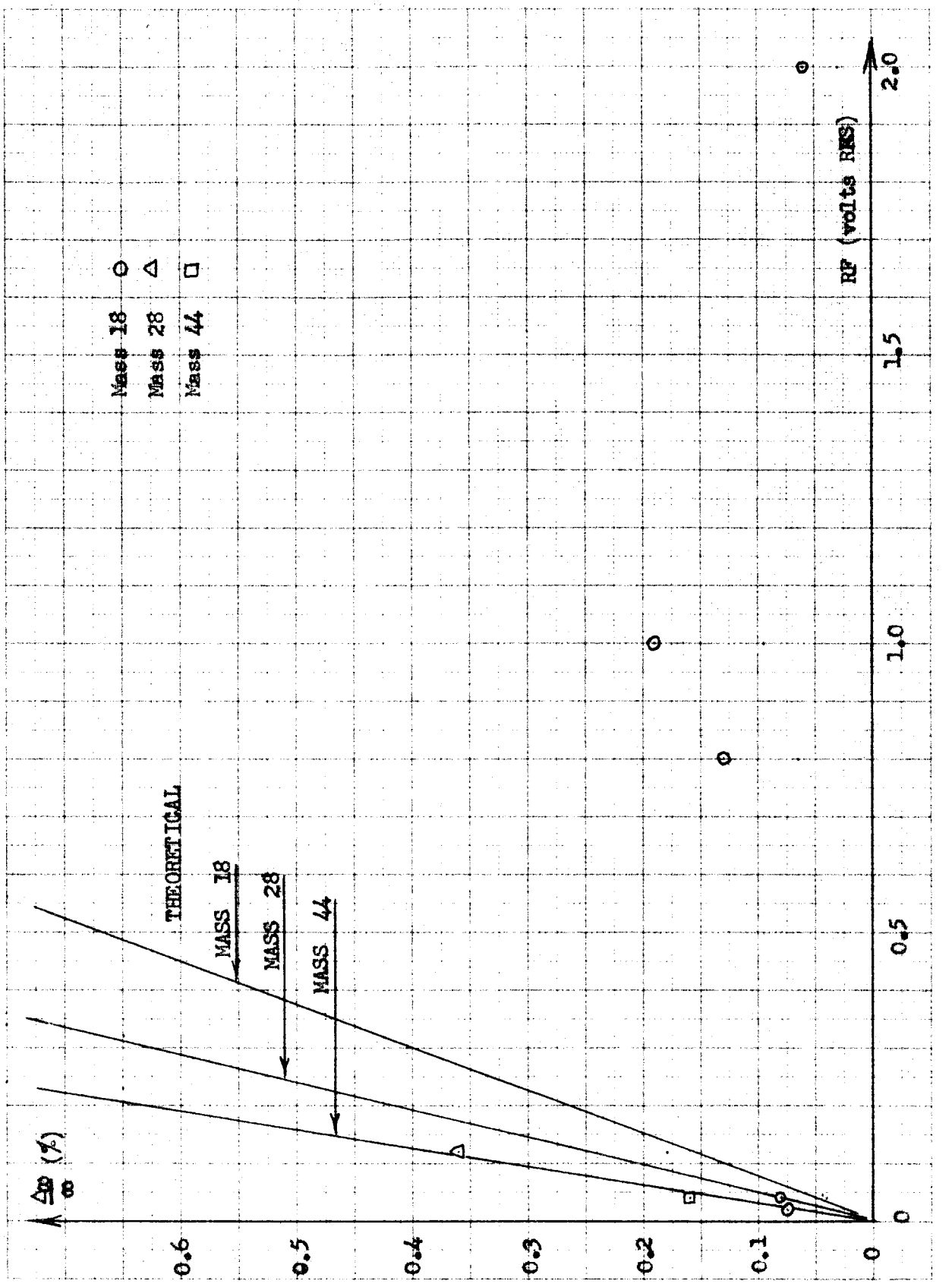

Fig. 42. Peak width versus RF.

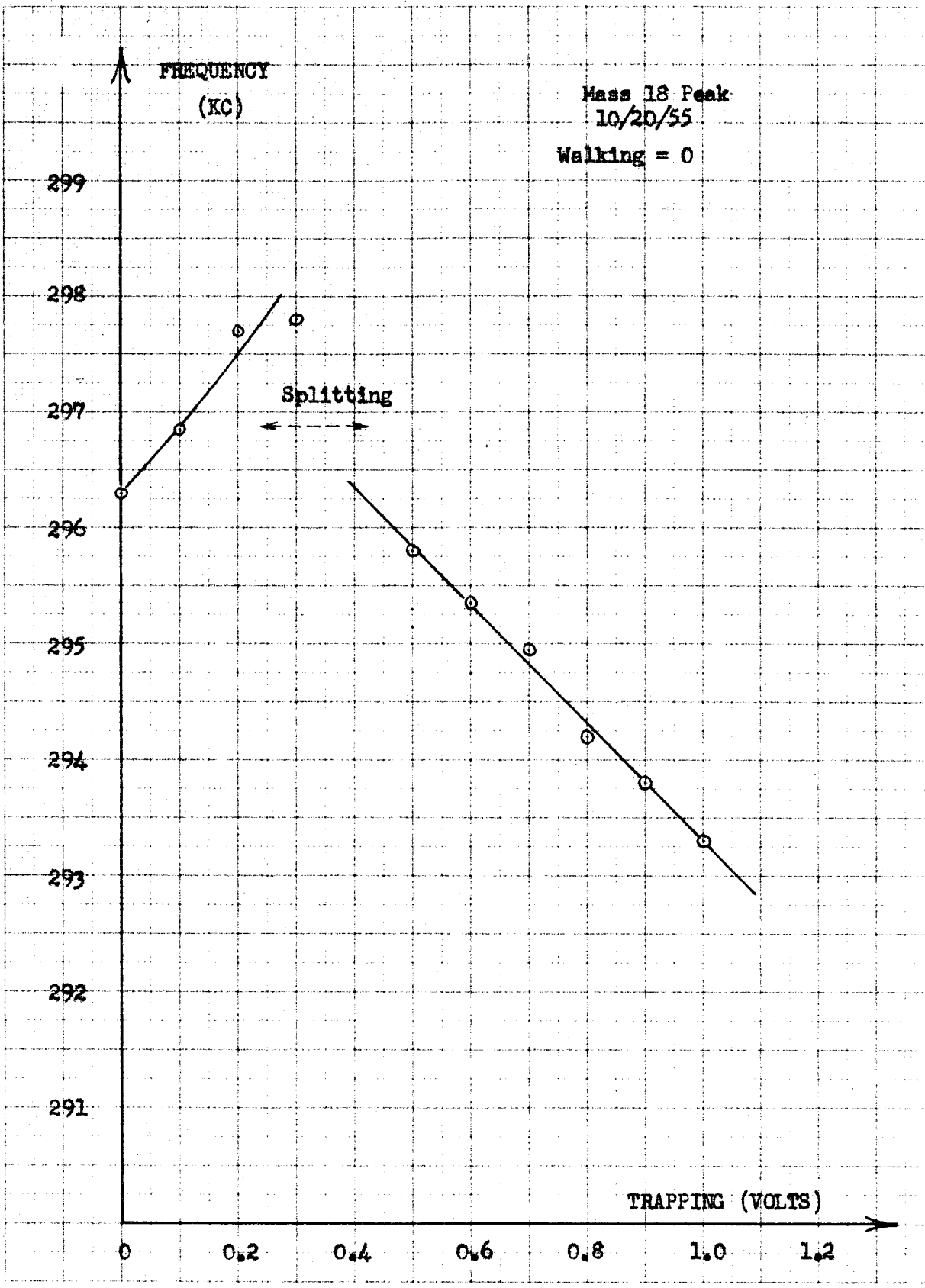

Fig. 43. Peak frequency versus trapping.

the rest is due to space charge effects.

The frequency of the peak is also affected by the RF and the electron beam current; but because of the difficulty in measuring the frequency, curves showing these effects were not taken.

Electron current. If space charge really is the important difficulty, and since it comes from ions which are produced by the electron beam, the electron current ought to be quite significant. And this was indeed found to be the case. Without trapping, an electron current of the order of 0.05 μamps was found to give maximum peak size. Above this current the peaks drop off in size, presumably from space charge effects, while below they again drop, but now from lack of ion production. This value of electron current and the collected ion current are roughly of the right order to be consistent with the known ion production of an electron beam. It is rather difficult to really pin this value down since nothing is known about the actual partial pressure for the water vapor in the background gas. With trapping, peak height was somewhat less dependent on electron current but still affected by it. This doesn't quite agree with the theory, but then the total space charge would undoubtedly be very sensitive to any walking voltages or any stray walking fields.

Mass 19 peak. One of the strongest pieces of evidence showing that there is a considerable amount of space charge in the Omegatron is the presence of the mass 19 peak. Normally, one would expect mass 18 (H_2O^+), mass 17 (HO^+) and mass 16 (O^+) . Fluorine has mass 19 and an isotope of argon has mass 38 (which might be double ionized) but both of these are extremely rare in the atmosphere and not generally

found in the background of a mass spectrometer. The only reasonable explanation of a 19 peak is that it is H_3O^+. This could be formed in a great variety of ways--e.g., ionization of an H_3O molecule formed in the collision of an H_2O^+ and an H^- or just the collision of an HO^+ with an H_2 -- and all the ways of forming H_3O require a collision of two or more molecules or ions. Normally in gaseous conduction the ions move without appreciable collisions, but in the Omegatron, especially with a small trapping applied, there is reason to suspect that it is difficult for the non-resonant ions to get out. In fact it appears that ions may slosh around in the space between the two end plates quite a while and that there may be a large concentration of these ions. Such a suggestion is strongly brought out in Fig. 44, where the upper trace shows normal mass 16, 17, 18 and 19 peaks with no trapping while the lower trace shows the same peaks with trapping (actual values, upper: RF = 3.5 volts, no trapping; lower: RF = 1.6, trapping = 0.4; sensitivity 10^{-14} amps/div). One would expect trapping to keep more ions around longer and thus make more H_3O^+, and Fig. 44 shows a relatively larger 19 peak for the case with trapping.

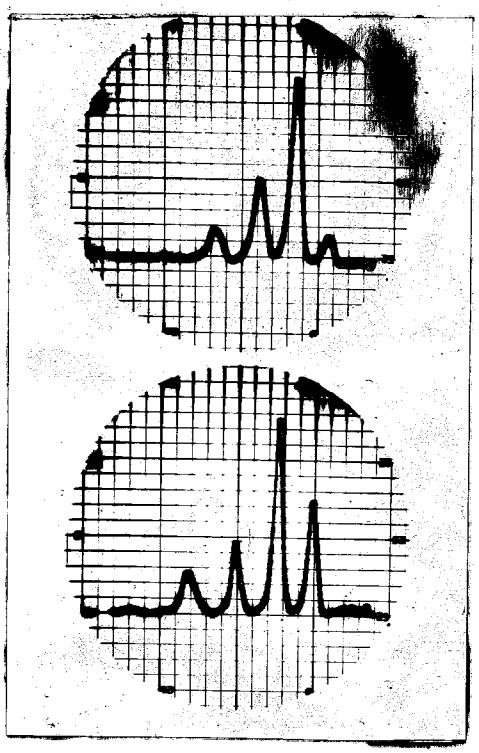

Fig. 44. Mass 19 Peak.

The application of a walking voltage, either plus or minus, generally reduced 19 more than 18. Of course, with sufficient walking all peaks were wiped out. Walking the ions away from the collector at a low enough rate so that a resonant 18 ion could still reach the collector apparently does not clear away the space charge fast enough; for the 19, while smaller, still persists.

An attempt was made to superimpose a fixed frequency RF field on the normal operation to remove a particular ion. It was hoped in this way to find which ions contributed to the mass 19 peak. The results were not too successful because of experimental difficulties, but it appeared that removing the mass 18 ions had the greatest effect on the 19 peak.

Anomalous behavior. Peak splitting is the most striking anomaly observed. Fig. 45 is a typical example of this characteristic. The upper trace shows a normal behavior for the mass 16, 17, 18, and 19 peaks at RF = 3.5 volts (sensitivity 5×10^{-14} amps/div). The lower trace shows the effect of 0.7 volts trapping with 2 volts of RF and no walking voltage, the peaks have all shifted to the right (lower frequency) and all appear to have a doublet character. No exact theoretical description of the cause of peak splitting has been found. Though it occurs under

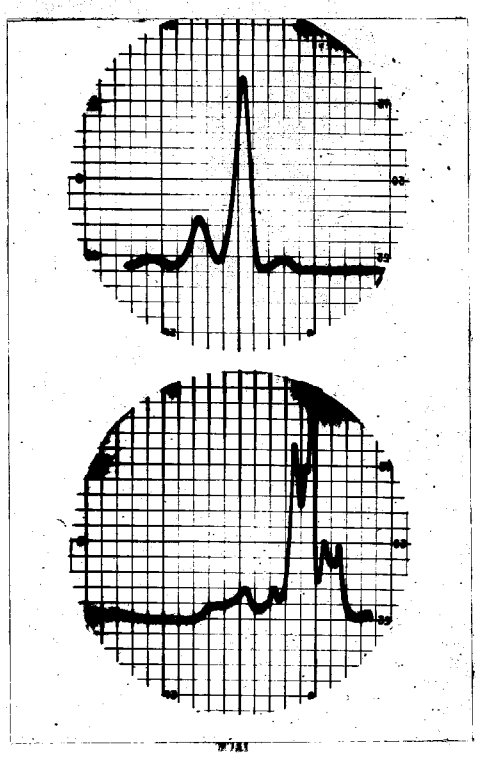

Fig. 45. Peak Splitting.

a variety of conditions, it always requires a fairly high trapping voltage and this strongly suggests that its primary cause is space charge. Generally a small amount of walking voltage eliminates any splitting. One can imagine several causes for splitting involving the actual detailed trajectory of an ion in going to the collector. Or it may be that when many ions are removed from the space charge near resonance, the change is significant enough to strongly affect their trajectories. In any event it seems pretty clear that splitting and space charge are rather intimately connected.

In the operation of the Omegatron, some difficulty was observed in getting completely reproducible results. Generally, results could be duplicated within 10 to 50%, depending on the quantity being measured. In addition, there were indications that several sweeps were required for a particular pattern to settle down on the oscilloscope. These effects can probably be explained in terms of surfaces charging up slightly, of variations in the actual composition of the background gas, and of deviations in the operating conditions, potentials, etc. Presumably the actual space charge and its distribution is quite sensitive to any stray potentials. None of these variations were sufficient to affect the general shape of the curves presented here or to change appreciably any of the conclusions drawn.

Some effect on peak size was observed when an external z field was applied. Slightly larger peaks were obtained with a z potential of about 0.1 volts in a particular direction. The effects were small enough to be of no great concern. Probably they can be explained in terms of field fringing around the exit hole for the electron beam from the slightly higher potential of the electron beam collector.

CHAPTER IV

CONCLUSIONS

In view of the theoretical and experimental work that has been described, the following conclusions can be drawn.

(a) An Omegatron built according to the standard procedures can be made an operating mass spectrometer. It will have several undesirable characteristics - requiring unusual voltages for good peaks, poorer resolution than expected, etc.

(b) In order to keep ions in the measuring region for a sufficient time, a trapping voltage must be applied. With trapping a positive space charge is guaranteed to build up. The space charge builds up to a value large enough to strongly influence the ion trajectories, peak frequency, width and height, and these effects are detrimental to good operation of the Omegatron. A small amount of walking voltage does indeed help to reduce the space charge effects, but it is not possible to apply enough walking to remove the space charge completely without at the same time eliminating the resonant ions themselves.

(c) Operation of the Omegatron without any trapping is possible, but high resolution cannot be obtained in this condition. The cause of this difficulty is a combination of effects from stray electric fields which both remove the resonant ions and make the space charge larger than one would normally expect. Again a walking field is not sufficient to overcome the difficulties.

These conclusions can effectively be summarized by saying that in

the Omegatron ions travel under the influence of very small electric fields and so it is difficult to keep them in a simple trajectory. Any small stray electric field or any small space charge forces can easily distort ion trajectories and spoil the operation.

As a result of these conclusions, it appears that the Omegatron as it stands will not make a good general purpose spectrometer. It should be very satisfactory though as a Helium leak detector where resolution and accuracy are not so important. Its simplicity and lack of critical slits to define a beam speak very strongly for it, particularly in this application.

Future work. Several ideas have suggested themselves toward eliminating some of the defects of the Omegatron. Basically, of course, one would like to get rid of the space charge completely, and one of the suggestions sounds as if it would do that. It might also be possible to work with the present system if some of the effects of the space charge could be reduced. Possible future work could be:

(a) RF detection. As a detector, an electrometer amplifier is a rather awkward device. It suffers from all the standard difficulties of DC amplifiers, such as drift and jumping, plus additional problems from the very high input resistance. An intriguing substitute for the electrometer, with the additional advantage that it might yield some information on the behavior of the ions near the origin, is an RF pick-up. This could, for example, be simply the Y plates in the present Omegatron. An ion traveling an almost circular path would induce an oscillating charge on the Y plates and this could be detected with an RF amplifier. Since the driving RF signal is push-pull, to first order it induces no voltage in the Y plates, and any small lack of symmetry

could be balanced out with an external balancing system. This type of detection is exactly the system used with nuclear resonance probes and seems to work very well there.

Considering a resonant ion traveling a circle of radius r, its y coordinate is $y = r \cos \omega t$. Such an ion induces an alternating charge on one of the Y plates of magnitude $q_{in} = (qr/a)\cos \omega t$, where q is the ion's charge and a is the plate spacing, and so the apparent RMS current flow between plates is $I_1 = \omega qr/a\sqrt{2}$. For a string of charges spiraling out with average radial velocity E/B and a total ion current I_i, the integrated effect of all the I_1's is $I = I_i(\omega Ba/8\sqrt{2}E)$. For mass 18 under the typical operating conditions, $I = 14\ I_i$, so the RMS RF current is about fifteen times the ion current.

In its simplest form, the RF amplifier input would be a tuned circuit connected between the Y plates. The mean square noise from the losses in the circuit is readily obtained by noting that the energy stored in the capacitor is $CV^2/2$ and by equipartition of thermal energy, the mean square energy must be $kT/2$. Thus $\overline{V_n^2} = kT/C$. The signal voltage developed across a tank resonant to ω by a current I would be $V_s = IR = IQ/\omega C$. Thus the signal to noise voltage ratio is

$$\frac{S}{N} = \frac{IQ}{\omega\sqrt{kTC}}$$

For $I = 10^{-12}$ amperes at room temperature with mass 18 under typical conditions and with $C = 20\ \mu\mu f$, $Q = 100$, this gives $S/N = 0.19$. This is clearly too small to be useful and in order to get anywhere at all the input would have to be a crystal. This would restrict operation

to a fixed frequency and so would require sweeping the magnetic field. Sweeping the magnetic field is desirable in many ways, but with the particular arrangement that was used in the experimental Omegatron, it could not be conveniently done and so this idea was not tried at all.

A feedback circuit arranged to increase the Q of an ordinary tank circuit might be considered in place of the crystal, but generally feedback does not improve the signal to noise ratio and if that rule applies here feedback would not help at all.

(2) Pulsed z field. One possibility for removing the space charge is to apply a pulsed z directed electric field. Short duration pulses could be used, and their repetition time made as long as possible. By using a large impulse for E_z, the ions can be given a very high velocity and all space charge cleared out in a negligible time. But during the time new ions are spiraling out to the collector, more space charge is forming. Typically, space charge is formed at a rate of about 10^{-12} amperes and a resonant ion takes about 66 μ sec to reach the collector. In this time a charge 66×10^{-12} coulombs builds up; or a line charge of 2.6×10^{-15} coul/m. This line charge is roughly 10^3 smaller than the amount necessary to significantly affect ion trajectories. Setting the repetition rate for the impulses to give a period roughly ten times the transit time of an ion would mean a collected ion current loss of about 10% over the maximum possible, which could be easily tolerated. In this time the line charge would build up to 2.6×10^{-14} coul/m, still tolerable. Thus this method should work for the conditions quoted, but these are rather low resolution conditions. With high resolution the transit time becomes longer, the impulse repetition rate must be slowed down, and the space charge

becomes larger. A factor of 100 increase in resolution would increase space charge by about the same amount, and this amount would be definitely significant. The conclusion is that while this method would help some, it would probably not be a cure all.

A brief effort was made to try this procedure out, but no success was obtained. The difficulty is in keeping the impulses out of the electrometer circuit where they block the input. Basically this is a simple circuit balancing problem but with large impulses it becomes quite sensitive.

(3) Dipole RF field. An extremely promising idea, the invention of Professor R.V. Langmuir, is to replace the uniform RF electric field with that of a dipole--a pair of wires parallel and close to the electron beam. The advantage of such a field is that it causes the resonant ions to spiral strongly at the beginning where the field is strong and so get away from the center area, and then to get their resolution further out where the field is weaker. Because the dipole field drops off so strongly with radius, it may be advantageous to superimpose a uniform RF electric field and so guarantee that ions continue to spiral outward. In such a case, the dipole field would really serve as an injector to a regular Omegatron. The presence of a DC grounded wire in the center would give a place for the non-resonant ions to go, and most of them would strike the wire very soon if it was reasonably large. The DC grounded wire would also fix the potential at the center and thus any space charge that did exist would have very little influence away from the center.

To avoid the effects of trapping field fringing on the resonant frequency, the use of alternating gradient (hard) focusing is suggested.

This is essentially using an AC potential on the trapping electrodes rather than DC, and a detailed analysis of such a potential leads to the conclusion that the net effect is indeed a trapping effect. Because the average fringing field from the trapping is zero, it is hoped that the ion resonant frequency would not be affected by it, but a more detailed analysis would be necessary to prove this.

No experiments have been made with the dipole RF field, but the hard focusing has been tried and shown to work successfully in the present Omegatron. As it stands it has no real advantage for the present Omegatron because it traps a large range of masses and so still leaves space charge.

(4) Selective trapping. A system which would trap only the resonant mass and untrap the remaining ones--essentially a spectrometer in a spectrometer--would clear up the space charge troubles. For example, such a system might be made with a DC untrapping voltage plus an AC hard focusing voltage. The combination of these two could be made trapping for a small range of masses only. This idea has not been tried at all.

Many other possibilities still exist for improving the operation of the Omegatron, and, of course, it must be remembered that it is a pretty good spectrometer as it stands.

APPENDIX I

The vectorial equation of motion for a mass-charge particle in a magnetic and electric field is

$$\bar{F} = m\,\bar{a} = q(\bar{v} \times \bar{B} + \bar{E}) \,. \qquad \text{AI-1}$$

Consider referring the motion to a coordinate system rotating about a fixed point with vector angular velocity $\bar{\omega}_s$. The total acceleration and velocity can be written in terms of the acceleration and velocity relative to the rotating coordinate system plus the coordinate systems angular velocity. This leads to

$$\bar{a} = \bar{a}_r + 2\bar{\omega}_s x \bar{v}_r + \bar{\omega}_s x(\bar{\omega}_s x \bar{r}) \qquad \text{AI-2}$$

and

$$\bar{v} = \bar{v}_r + \bar{\omega}_s x \bar{r} \,, \qquad \text{AI-3}$$

where the subscript r refers to relative motion. In AI-2, the second term on the right is the Coriolis acceleration, while the third term is the centripetal acceleration. Using AI-2 and AI-3 in AI-1 gives

$$m(\bar{a}_r + 2\bar{\omega}_s x \bar{v}_r + \bar{\omega}_s x(\bar{\omega}_s x \bar{r})) = q(\bar{v}_r x \bar{B} + (\bar{\omega}_s x \bar{r}) x \bar{B} + \bar{E}) \,. \qquad \text{AI-4}$$

This can be rewritten as

$$m\bar{a}_r = q\left[\bar{v}_r x(\bar{B} + 2\,\frac{m}{q}\,\bar{\omega}_s) + (\bar{\omega}_s x \bar{r}) x(\bar{B} + \frac{m}{q}\,\bar{\omega}_s) + \bar{E}\right] \,. \qquad \text{AI-5}$$

There are now three cases of interest; (a) $\bar{\omega}_s = -(q/2m)\bar{B}$ for which the first term on the right of AI-5 disappears, (b) $\bar{\omega}_s = \bar{\omega}$, where $\bar{\omega}$ is the vector electric field frequency, which makes the electric field stationary in the rotating coordinate system, and (c) $\bar{\omega}_s = (q/m)\bar{B}$ for which the second term on the right disappears.

(a) $\bar{\omega}_s = -(q/2m)\bar{B}$. In this case, AI-5 becomes

$$m\bar{a}_r = q\left[-(q/4m)(\bar{B}x\bar{r})x\bar{B} + \bar{E}\right]. \qquad \text{AI-6}$$

In the particular case that $\bar{r}$ is confined to the plane perpendicular to $\bar{B}$ and $\bar{\omega}_s$ (as it is in the actual Omegatron problem), this becomes

$$\begin{aligned} m\bar{a}_r &= q\left[-(q/4m)B^2\,\bar{r} + \bar{E}\right] \\ &= -m(qB/2m)^2\,\bar{r} + q\bar{E} \\ &= -m\,\omega_c^2\,\bar{r}/4 + q\bar{E} \end{aligned} \qquad \text{AI-7}$$

where $\omega_c = qB/m$. In these equations, the scalar B is simply the magnitude of the vector $\bar{B}$.

(b) $\bar{\omega}_s = \bar{\omega}$. In this case, AI-5 is unchanged except for replacing $\bar{\omega}_s$ by $\bar{\omega}$, thus

$$m\bar{a}_r = q\left[\bar{v}_r x(\bar{B} + 2\,\frac{m}{q}\,\bar{\omega}) + (\bar{\omega}x\bar{r})x(\bar{B} + \frac{m}{q}\,\bar{\omega}) + \bar{E}\right]. \qquad \text{AI-8}$$

If the electric field rotates in the plane perpendicular to the magnetic field, then $\bar{\omega}$ and $\bar{B}$ are parallel. There is still a plus or minus sign to be specified depending on whether they point in the same or opposite directions, but this can be taken care of by defining

$$\bar{\omega} = -(\omega/B)\,\bar{B} \quad , \qquad \text{AI-9}$$

where B is still the magnitude of $\bar{B}$ and so is always positive. The scalar ω has a magnitude equal to the magnitude of the vector $\bar{\omega}$ and a sign which depends on the relative direction of $\bar{\omega}$ and $\bar{B}$ (plus if they are opposite). The sign convention here is chosen to make ω normally a positive number. Using AI-9, AI-8 becomes

$$m\bar{a}_r = q\left[(1 - 2\omega/\omega_c)\,\bar{v}_r x\bar{B} - (1 - \omega/\omega_c)(\omega/B)(\bar{B}x\bar{r})x\bar{B} + \bar{E}\right]. \quad \text{AI-10}$$

If $\bar{r}$ is again restricted to the plane perpendicular to $\bar{B}$ and $\bar{\omega}$, this can be written as

$$m\bar{a}_r = q\left[(1 - 2\omega/\omega_c)\bar{v}_r x\bar{B} + \bar{E}\right] - q(1 - \omega/\omega_c)\,\omega B\bar{r}$$

$$= q\left[(1 - 2\omega/\omega_c)\bar{v}_r x\bar{B} + \bar{E}\right] - m\omega(\omega_c - \omega)\,\bar{r} \quad . \quad \text{AI-11}$$

If $\bar{B}_1 = \bar{B}(1 - 2\omega/\omega_c)$ and $K = m\omega(\omega_c - \omega)$, this can be reduced to

$$m\bar{a}_r = q(\bar{v}_r x\bar{B}_1 + \bar{E}) - K\,\bar{r} \quad . \quad \text{AI-12}$$

(c) $\bar{\omega}_s = -(q/m)\bar{B}$. In this case, AI-5 becomes simply

$$m\bar{a}_r = q(-\bar{v}_r x\bar{B} + \bar{E}) \quad . \quad \text{AI-13}$$

In case (c) it is clear that if the electric field is zero, a particle can be stationary in the rotating coordinate system and satisfy AI-13. In the fixed coordinate system its motion is circular, with vector angular frequency $-q\bar{B}/m$ (called the cyclotron resonance frequency). Vectorially then the cyclotron resonance frequency is $\bar{\omega}_c = -q\bar{B}/m$.

Referring to Fig. 9 (page 17) in the body of this report, the angular frequency $\bar{\omega}$ and the direction of $\bar{B}$ are defined consistently with AI-9, and furthermore $\bar{\omega}_s$ is defined opposite in direction to $\bar{B}$. In view of this, the three cases considered here can be described as (a) $\omega_s = \omega_c/2$, (b) $\omega_s = \omega$ and (c) $\omega_s = \omega_c$, which is the way they are listed in the text. Equation AI-7 then becomes II-7, AI-12 becomes II-8, and AI-13 becomes II-10.

APPENDIX II

This appendix contains a curve showing the air gap flux density as a function of the coil current for the electromagnet that was used. This curve is Fig. 46 on the next page. It is included here for the convenience of anyone who might want to use this experimental setup again in the future.

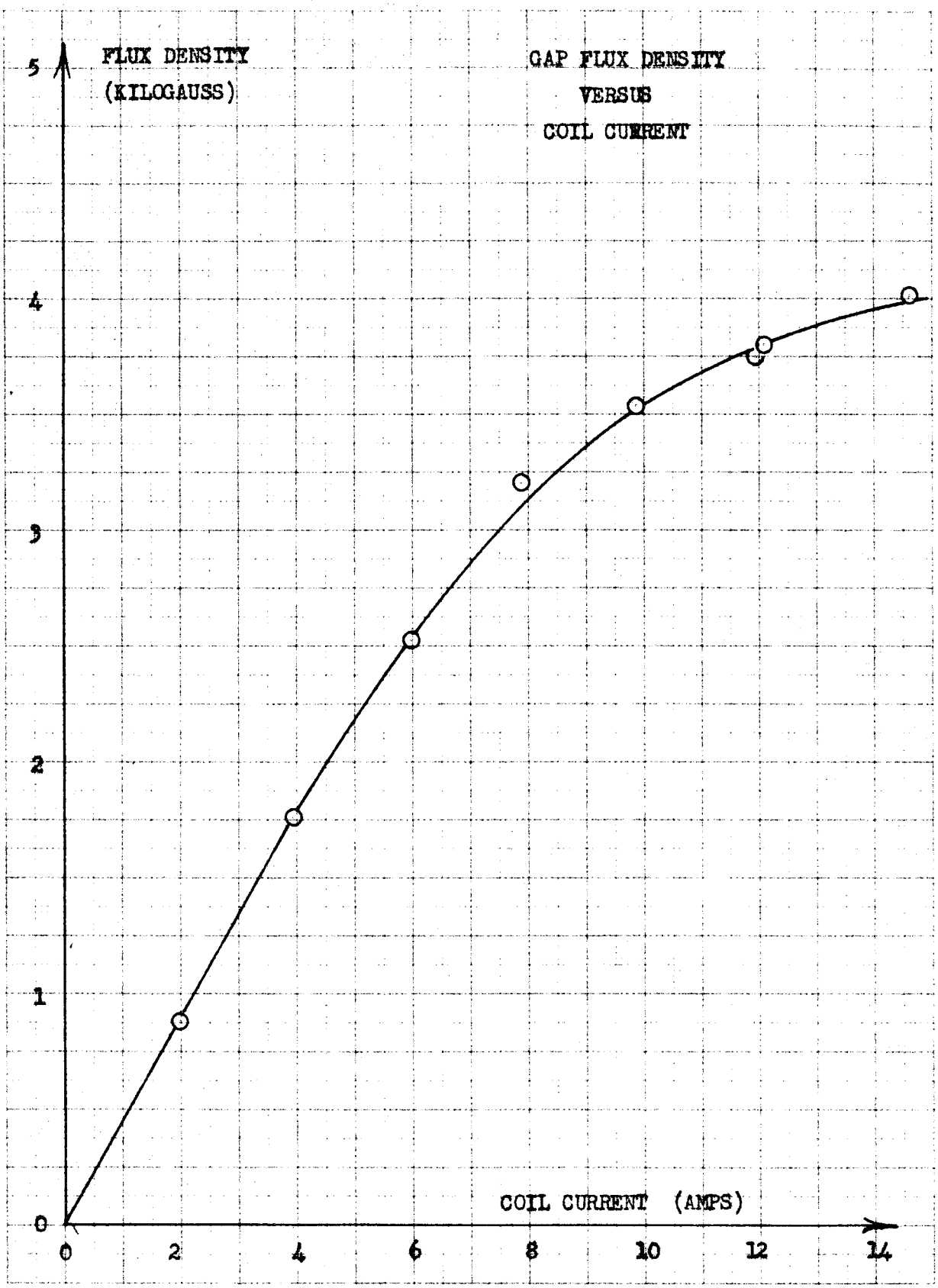
FLUX DENSITY
(KILOGAUSS)
GAP FLUX DENSITY
VERSUS
COIL CURRENT
5
4
3
2
1
0
COIL CURRENT (AMPS)
0
2
4
6
8
10
12
14

Fig. 46.

APPENDIX III

This appendix contains detailed circuit diagrams for the RF part of the system and for the electrometer amplifier. The equipment described was built specifically for operation with the experimental Omegatron. Fig. 47 shows the circuit for the 10.5 MC fixed frequency oscillator, while Fig. 48 shows the mixer-amplifier used to produce the low frequency sweep signal. Fig. 49 shows the circuit diagram for the electrometer amplifier.

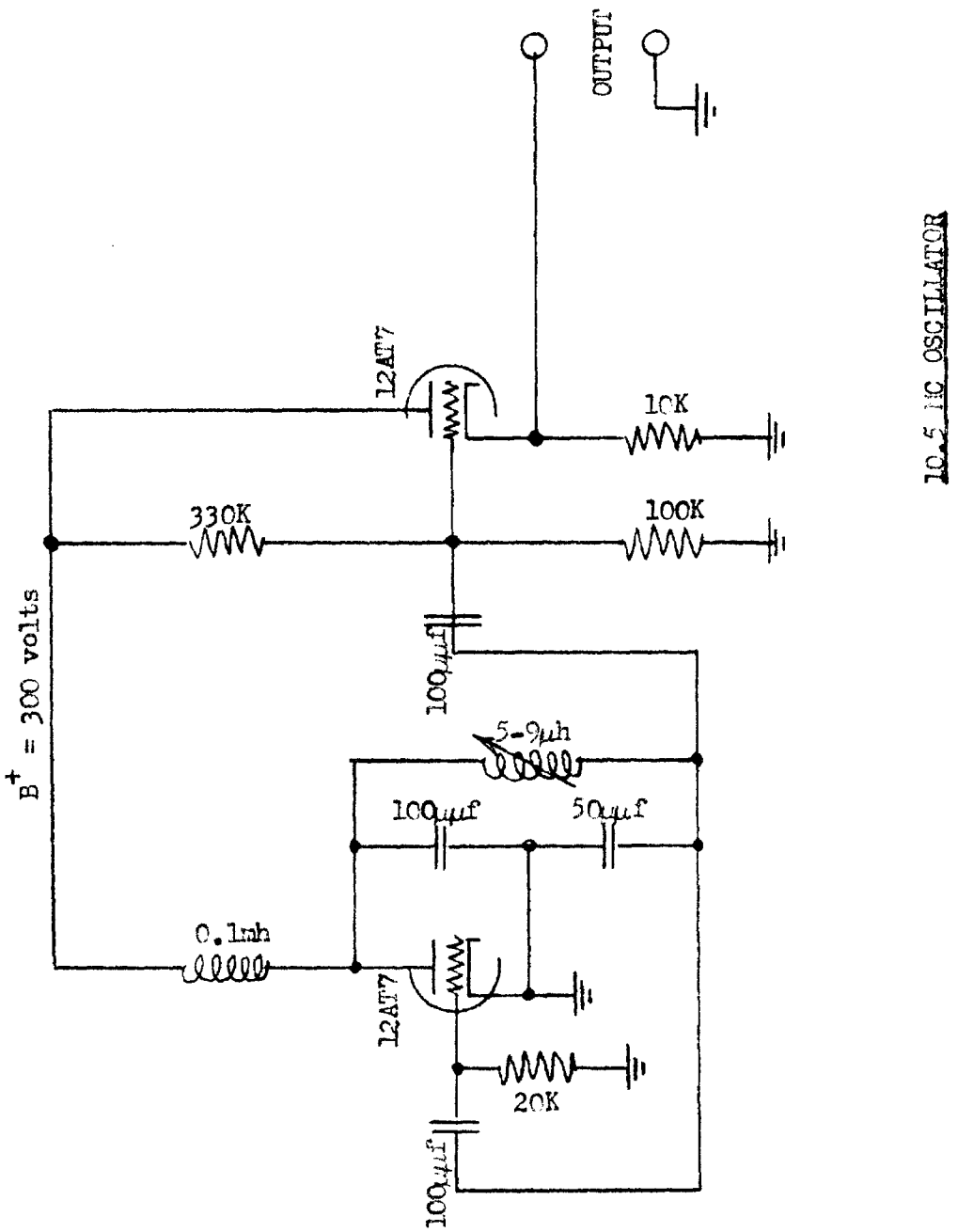

Fig. 47. Oscillator.

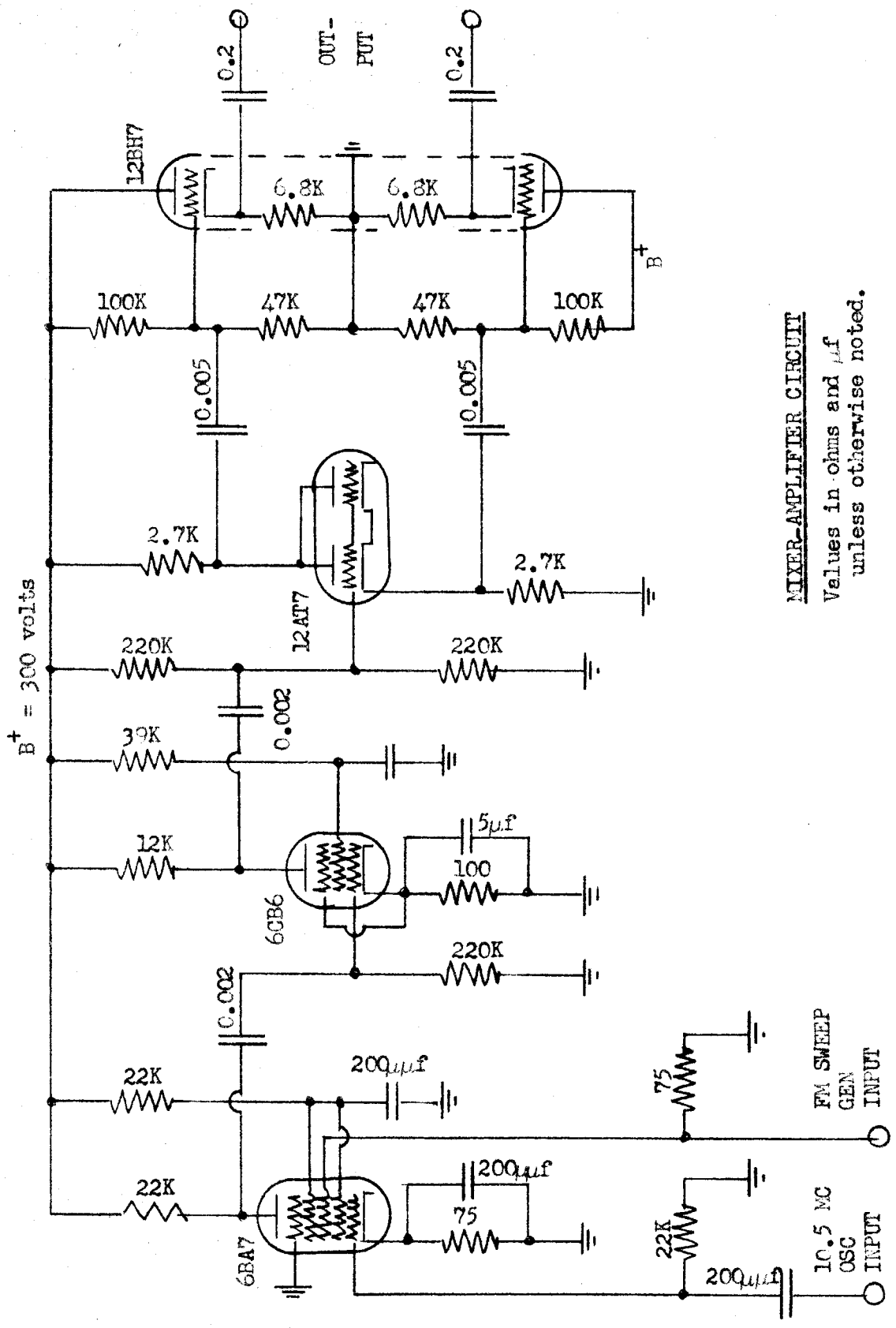

Fig. 48. Mixer-amplifier.

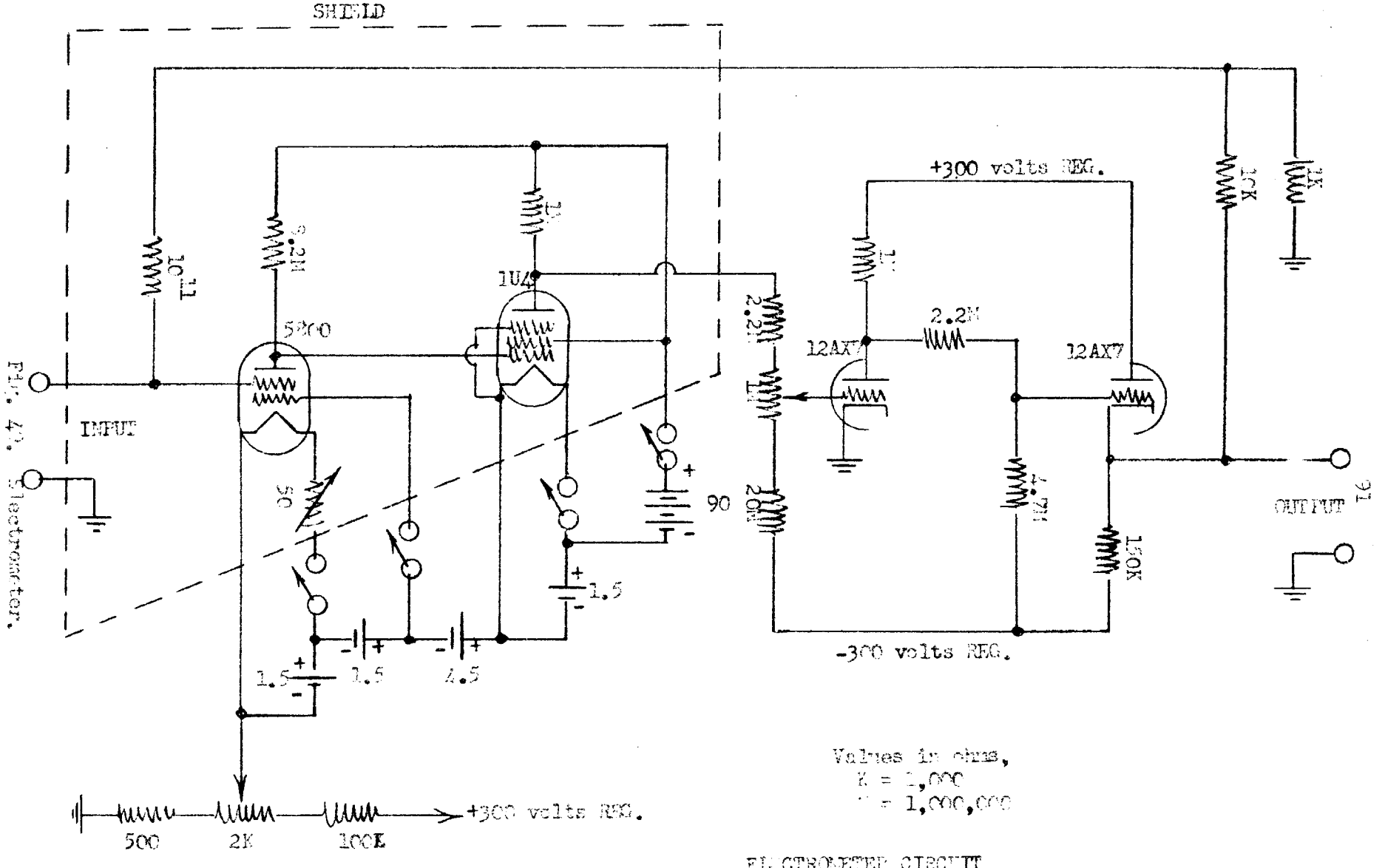

Values in ohms,
K = 1,000
M = 1,000,000

ELECTROMETER CIRCUIT

REFERENCES

1. Hipple, J.A., Sommer, H. and Thomas, H.A., Phys. Rev. 76:1877 (1949), 78:332 (1950).
2. Sommer, H., Thomas, H.A. and Hipple, J.A., Phys. Rev. 82:697 (1951).
3. Bell, R.L., Services Electronics Res. Labs. Tech. Jour. 5:39 (1955).
4. Alpert, D. and Buritz, R.S., J. App. Phys. 25:202 (1954).
5. Edwards, A.G., Brit. J. App. Phys. 6:44 (1955).
6. Thomson, J.J., "Positive Rays of Electricity" Longmans Green, N.Y. 2nd ed., 1921.
7. Aston, F.W., "Mass-spectra and Isotopes" Longmans Green, N.Y. 1933.
8. Dempster, A.J., Phys. Rev. 11:316 (1918), 18:415 (1921), 20:631 (1922).
9. Bainbridge, K.T., J. Frank. Inst. 215:509 (1933).
10. Bleakney, W. and Hipple, J.A., Phys. Rev. 53:521 (1938).
11. Inghram, M.G. and Hayden, R.J., "A Handbook on Mass Spectroscopy" National Academy of Sciences - National Research Council 1954.
12. Segre, E. "Experimental Nuclear Physics" Vol. 1, Wiley 1953.
13. Robertson, A.J.B., "Mass Spectrometry" Wiley, N.Y. 1954.
14. Smythe, W.R., Rumbaugh, L.H. and West, S.S., Phys. Rev. 45:724 (1934).
15. Smythe, W.R., and Hemmendinger, A., Phys. Rev. 51:178 (1937).
16. Nier, A.O., Phys. Rev. 52:933 (1937).
17. Nier, A.O., Rev. Sci. Instr. 11:212 (1940).
18. Hipple, J.A., J. App. Phys. 13:551 (1942).
19. Ewald, H., Z. Naturforsch. 1:131 (1946).
20. Nier, A.O. and Roberts, T.R., Phys. Rev. 81:507 (1951).
21. Yates, E.L., Pro. Roy. Soc. London A168:148 (1938).
22. Oliphant, M.L., Shire, E.S. and Crowther, B.M., Pro. Roy. Soc. London A146:922 (1934).

23. Smythe, W.R., Phys. Rev. 28:1275 (1926).

24. Smythe, W.R. and Mattauch, J., Phys. Rev. 40:429 (1932).

25. Glenn, W.E., UCRL Report No. 1628 (1952).

26. Keller, R., Helv. Phys. Acta 22:386 (1949).

27. Cameron, A.E. and Eggers, D.F., Rev. Sci. Instr. 19:605 (1948).

28. Goudsmit, S.S., Phys. Rev. 74:622 (1948).

29. Smith, L.G., Rev. Sci. Instr. 18:540 (1947).

30. Berry, C.E., J. of App. Phys. 25:28 (1954).

31. Stoker, J.J., "Nonlinear Vibrations" Interscience Publishers Inc. N. Y., 1950.

32. Tonks, L. and Langmuir, I., Phys. Rev. 34:896 (1929).

33. Langmuir, I., J. Frank. Inst. 214:275 (1932).

34. Compton, K.T. and Langmuir, I., Revs. Mod. Phys. 2:123 (1930).

35. Berry, C. E., Phys. Rev. 78:597 (1950).